NASA
Reference
Publication
1303

May 1993

A Shadowgraph Study of Two Proposed Shuttle-C Launch Vehicle Configurations

A. M. Springer
and D. C. Pokora

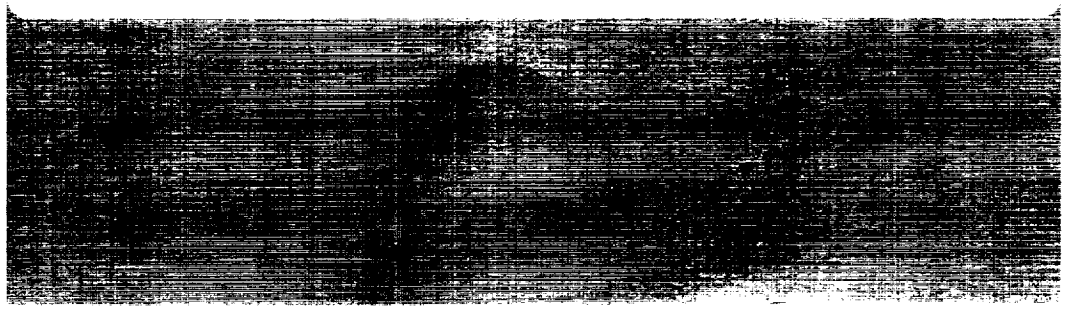

NASA

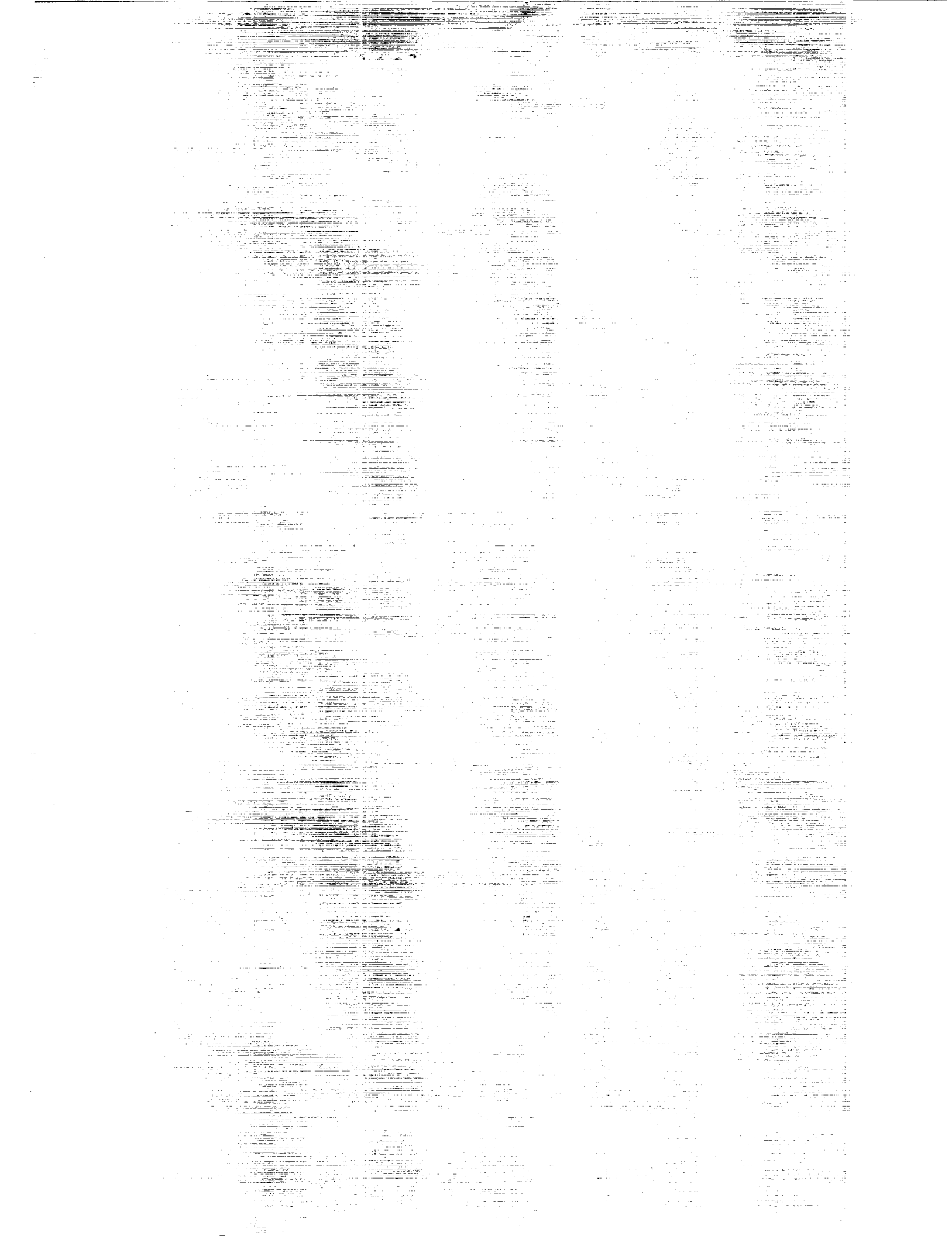

NASA Reference Publication 1303

1993

A Shadowgraph Study of Two Proposed Shuttle-C Launch Vehicle Configurations

A. M. Springer
and D. C. Pokora
George C. Marshall Space Flight Center
Marshall Space Flight Center, Alabama

National Aeronautics and Space Administration

Office of Management

Scientific and Technical Information Program

ACKNOWLEDGMENTS

The authors would like to acknowledge the wind tunnel test team of Marshall Space Flight Center. They were instrumental in running the wind tunnel test and the installation of the shadowgraph system. A sincere thanks to H. Brewster, A. Frost, and C. Dill.

TABLE OF CONTENTS

		Page
I.	INTRODUCTION	1
II.	MODEL AND FACILITY DESCRIPTION	1
	A. Facility Description	1
	B. Model Description	1
	C. Shadowgraph System	2
III.	SHADOWGRAPH DESCRIPTION	2
IV.	CONCLUSIONS	3
REFERENCES		4

LIST OF ILLUSTRATIONS

Figure	Title	Page
1.	NASA MSFC's 14- by 14-in trisonic wind tunnel	5
2.	Shuttle-C reference configuration installed in the MSFC 14-in wind tunnel (TWT 715)	6
3.	Shuttle-C cargo carrier configurations mated to lower stack	7
4.	Sketch of shadowgraph setup	8
5.	Reference configuration Mach 1.46, alpha = –4, beta = 0	9
6.	Reference configuration Mach 0.90, alpha = 0, beta = 0	12
7.	Reference configuration Mach 0.90, alpha = -4, beta = 0	12
8.	Reference configuration Mach 0.95, alpha = 0, beta = 0	13
9.	Reference configuration Mach 0.95, alpha = -4, beta = 0	13
10.	Reference configuration Mach 1.05, alpha = 0, beta = 0	14
11.	Reference configuration Mach 1.05, alpha = -4, beta = 0	14
12.	Reference configuration Mach 1.10, alpha = 0, beta = 0	15
13.	Reference configuration Mach 1.10, alpha = -4, beta = 0	15
14.	Reference configuration Mach 1.25, alpha = 0, beta = 0	16
15.	Reference configuration Mach 1.25, alpha = -4, beta = 0	16
16.	Reference configuration Mach 1.46, alpha = 0, beta = 0	17
17.	Reference configuration Mach 1.46, alpha = -4, beta = 0	17
18.	Reference configuration Mach 1.96, alpha = 0, beta = 0	18
19.	Reference configuration Mach 1.96, alpha = -4, beta = 0	18
20.	Reference configuration Mach 2.74, alpha = 0, beta = 0	19
21.	Reference configuration Mach 2.74, alpha = -4, beta = 0	19
22.	Reference configuration Mach 3.48, alpha = 0, beta = 0	20

LIST OF ILLUSTRATIONS (Continued)

Figure	Title	Page
23.	Reference configuration Mach 3.48, alpha = -4, beta = 0	20
24.	Reference configuration Mach 4.95, alpha = 0, beta = 0	21
25.	Reference configuration Mach 4.95, alpha = -4, beta = 0	21
26.	Reference configuration Mach 0.90, alpha = 0, beta = 0, roll = 90°	24
27.	Reference configuration Mach 0.95, alpha = 0, beta = 0, roll = 90°	24
28.	Reference configuration Mach 1.05, alpha = 0, beta = 0, roll = 90°	25
29.	Reference configuration Mach 1.10, alpha = 0, beta = 0, roll = 90°	25
30.	Reference configuration Mach 1.25, alpha = 0, beta = 0, roll = 90°	26
31.	Reference configuration Mach 1.46, alpha = 0, beta = 0, roll = 90°	26
32.	Reference configuration Mach 1.96, alpha = 0, beta = 0, roll = 90°	27
33.	Reference configuration Mach 2.74, alpha = 0, beta = 0, roll = 90°	27
34.	Reference configuration Mach 3.48, alpha = 0, beta = 0, roll = 90°	28
35.	Reference configuration Mach 4.95, alpha = 0, beta = 0, roll = 90°	28
36.	CYL-92-26-MV configuration Mach 0.90, alpha = 0, beta = 0	30
37.	CYL-92-26-MV configuration Mach 0.95, alpha = 0, beta = 0	31
38.	CYL-92-26-MV configuration Mach 0.95, alpha = -4, beta = 0	31
39.	CYL-92-26-MV configuration Mach 1.05, alpha = 0, beta = 0	32
40.	CYL-92-26-MV configuration Mach 1.05, alpha = -4, beta = 0	32
41.	CYL-92-26-MV configuration Mach 1.10, alpha = 0, beta = 0	33
42.	CYL-92-26-MV configuration Mach 1.10, alpha = -4, beta = 0	33
43.	CYL-92-26-MV configuration Mach 1.25, alpha = 0, beta = 0	34
44.	CYL-92-26-MV configuration Mach 1.25, alpha = -4, beta = 0	34

LIST OF ILLUSTRATIONS (Continued)

Figure	Title	Page
45.	CYL-92-26-MV configuration Mach 1.46, alpha = 0, beta = 0	35
46.	CYL-92-26-MV configuration Mach 1.46, alpha = -4, beta = 0	35
47.	CYL-92-26-MV configuration Mach 1.96, alpha = 0, beta = 0	36
48.	CYL-92-26-MV configuration Mach 2.74, alpha = 0, beta = 0	37
49.	CYL-92-26-MV configuration Mach 2.74, alpha = -4, beta = 0	37
50.	CYL-92-26-MV configuration Mach 3.48, alpha = 0, beta = 0	38
51.	CYL-92-26-MV configuration Mach 3.48, alpha = -4, beta = 0	38
52.	CYL-92-26-MV configuration Mach 4.95, alpha = 0, beta = 0	39
53.	CYL-92-26-MV configuration Mach 4.95, alpha = -4, beta = 0	39

REFERENCE PUBLICATION

A SHADOWGRAPH STUDY OF TWO PROPOSED SHUTTLE-C LAUNCH VEHICLE CONFIGURATIONS

I. INTRODUCTION

This report, the first in a series of shadowgraph studies of various launch vehicle configurations, presents shadowgraphs of two proposed Shuttle-C configurations for the trisonic Mach range of 0.6 to 5.0. Shadowgraphs at angles-of-attack of 0° and −4° and roll angles of 90° are shown for the majority of the Mach range. These shadowgraphs present a pictorial view of the flow fields over the Shuttle-C configurations. These configurations were tested in the Marshall Space Flight Center's (MSFC's) 14-in trisonic wind tunnel over the period of October 1988 to February 1989.[1]

This report presents shadowgraphs for the Shuttle-C vehicle in a concise format, offers a means of easy transfer of the data to interested parties, and documents the results for future study.

II. MODEL AND FACILITY DESCRIPTION

A. Facility Description

The MSFC 14- by 14-in trisonic wind tunnel is an intermittent blowdown tunnel which operates by high pressure air flowing from storage to either vacuum or atmosphere conditions. The transonic test section, with variable porous walls, provides a Mach number range from 0.2 to 2.0. A solid-wall supersonic test section provides the entire range from 2.74 to 5.0 with one set of automatically actuated contour blocks. Downstream of the test section is a hydraulically controlled pitch sector that provides the capability of testing up to 20 angles-of-attack from −10° to +10° during each run. Sting offsets are available for obtaining various maximum angles-of-attack up to 90°. This is further detailed in reference 2. The MSFC 14- by 14-in trisonic wind tunnel facility is shown in figure 1.

B. Model Description

The 0.004 scale Shuttle-C models consisted of two cargo carrier (CC) configurations mated to the space transportation system (STS) lower stack and an external tank (ET) with two solid rocket boosters (SRB's). The CC models were representations of the Shuttle-C sidemount concepts studied. These models consisted of a cylindrical-shaped forward body with an STS boattail. The reference configuration was a cylindrical body of 82-ft length and 18.3-ft (full scale) diameter. The nose was a 26.5° half-angle nose cone that was blunted with a nose radius of 3.542 ft (full scale). The orbital maneuvering system (OMS) pods were mounted in the same relative position as they are on the STS orbiter. Figure 2 shows the reference configuration mounted in the trisonic wind tunnel. Another configuration tested was identical to the reference configuration but the forward cylinder was extended to 92 ft (full scale). Figure 3 is a comparison sketch of the two configurations. Shadowgraphs were taken for these two configurations.

C. Shadowgraph System

The 14-in wind tunnel's shadowgraph system consists of a spark source, multiple film holders, and a mounting bracket for the holders. The spark source is mounted on one side with the mounting bracket/film holder on the other side of the test section. Glass wall inserts are installed in the transonic test section, while the supersonic test section has conventional windows. The spark source is fired, exposing the film, thus producing a shadowgraph. Figure 4 shows a sketch of the shadowgraph setup.

Without flow, the spark source shines through the test section containing stagnant air and illuminates the film with uniform intensity. When the tunnel is started and flow passes through the test section, the light beam will be refracted wherever there is a density gradient. A constant gradient, an empty test section, will result in every light ray being refracted evenly, producing no change on the film. Only if there is a variation in the density gradient will the light from the spark source converge or diverge. A picture of the instantaneous density gradients is shown on the film when the spark source is fired. The shadowgraph easily allows shock waves to be seen. A density gradient is positive upstream of the shock and negative downstream. The shadowgraph film shows the shock wave as a dark line followed by a white line.

The shadowgraph system used for the 14-in wind tunnel is explained in detail in reference 3. Reference 3 also explains the theory behind the system and the supporting tests done to initially verify the system. This reference also explains the effects of the glass walls on the shadowgraph. This appears on the shadowgraph to look something like cross hatching in the subsonic and sonic Mach range. Currently only the single-film method, not the multiple-exposure roll which is also shown in reference 3, is used. Kodak Tri-X 8- by 20-in, black and white, pan professional film is used for the shadowgraphs.

III. SHADOWGRAPH DESCRIPTION

The shadowgraph is a flow visualization technique that shows the second spatial derivative of the density field or the gradient of the density gradient. The shadowgraph is used to show boundary layers, flow separation, and shock wave formations. All flow visualization techniques are dependent on variation in the flow fields density. An interferometer measures the density level with regards to a reference. The fringe shifts are counted to obtain the density variations. A Schlieren system shows the gradient in density or the first x derivative. The shadowgraph system is easy to use and the relative shock strengths are easily seen, but the actual density levels cannot be obtained.

Boundary layers and separated regions are easily seen in shadowgraphs if the flow field density is not too low. The density changes across shocks, and expansions waves are governed by the ratios which are functions of Mach number and flow direction. The density gradients of the flow are dependent on the ratios of upstream and downstream flow fields. This dependence results in low-density flow fields not being as clear as high-density flow in the shadowgraphs. The shadowgraph system and its relation to other optical flow methods are discussed in reference 4. Further details concerning shadowgraphs and their application to launch vehicle aerodynamic study are found in reference 5.

These visual representations of the flow are used in the venting analysis and aerodynamic analysis of the vehicle.

IV. CONCLUSIONS

Shadowgraphs are presented for the trisonic range of Mach numbers for two proposed Shuttle-C configurations. The shadowgraphs show the effects of Mach number, angle of attack, angle of sideslip, and cargo carrier configuration. The shadowgraphs presented are of great use in the analysis of the aerodynamic characteristics for the presented configurations.

The Shuttle-C configuration is a multibody side-mounted configuration, like the shuttle. This type configuration results in significant interactions between the components. Part of the interaction between components is due to the interaction of the bow shock waves off each of the components. This can be seen in figure 32 and 18, a top and side view of the reference configuration.

The effects of the differences in configuration, i.e., payload bay length, can be seen in these shadowgraphs. The flow fields are generally the same for both configurations. The Shuttle-C cargo carrier nose or bow shock wave is moved forward on the 92-ft length payload model (fig. 45) as compared to the reference configuration (fig. 16). This moves the shock impingement point on the ET and changes the interference patterns between the cargo carrier and the lower stack.

In general, shock waves seen at lower Mach numbers appear as vertical lines forward of the vehicle. As Mach number increases, a shock wave traverses the vehicle and changes from the appearance of a vertical line, a normal shock, to that of an oblique line, an oblique shock.

At the higher Mach numbers, the shadowgraphs appear to be clearer and shock waves more pronounced. This is due to the larger density variation fore and aft of the shock.

The flow phenomena around the reference configuration, as seen in a typical shadowgraph, is shown in figure 5. This figure is the same shadowgraph as figure 17, but with the major points of the flow field highlighted.

REFERENCES

1. Pokora, D.C.: "Posttest report for the Shuttle-C Test in the MSFC 14-Inch Trisonic Wind Tunnel (TWT 715)." ED35-17-89, February 28, 1989.

2. Simon, E.H.: "The George C. Marshall Space Flight Center's 14x14 Inch Trisonic Wind Tunnel Technical Handbook." NASA TMX-64624, November 5, 1971.

3. Clark, J., Heaman, J.P., and Stewart, D.L.: "14-Inch Wind Tunnel Spark Shadowgraph System." NASA TM X-53196, January 22, 1965.

4. Shapiro, A.H.: "The Dynamics and Thermodynamics of Compressible Fluid Flow Volume I." John Wiley and Sons, Inc., 1953, Chapter 3.7. Optical Methods of Investigation, p. 59–68.

5. Andrews, C.D., and Carlson, D.R.: "Shadowgraph Study of the Upper Stage Flow Fields of Some Saturn V Study Configurations in the Transonic Mach Number Range." NASA TN D-2755, April 1965.

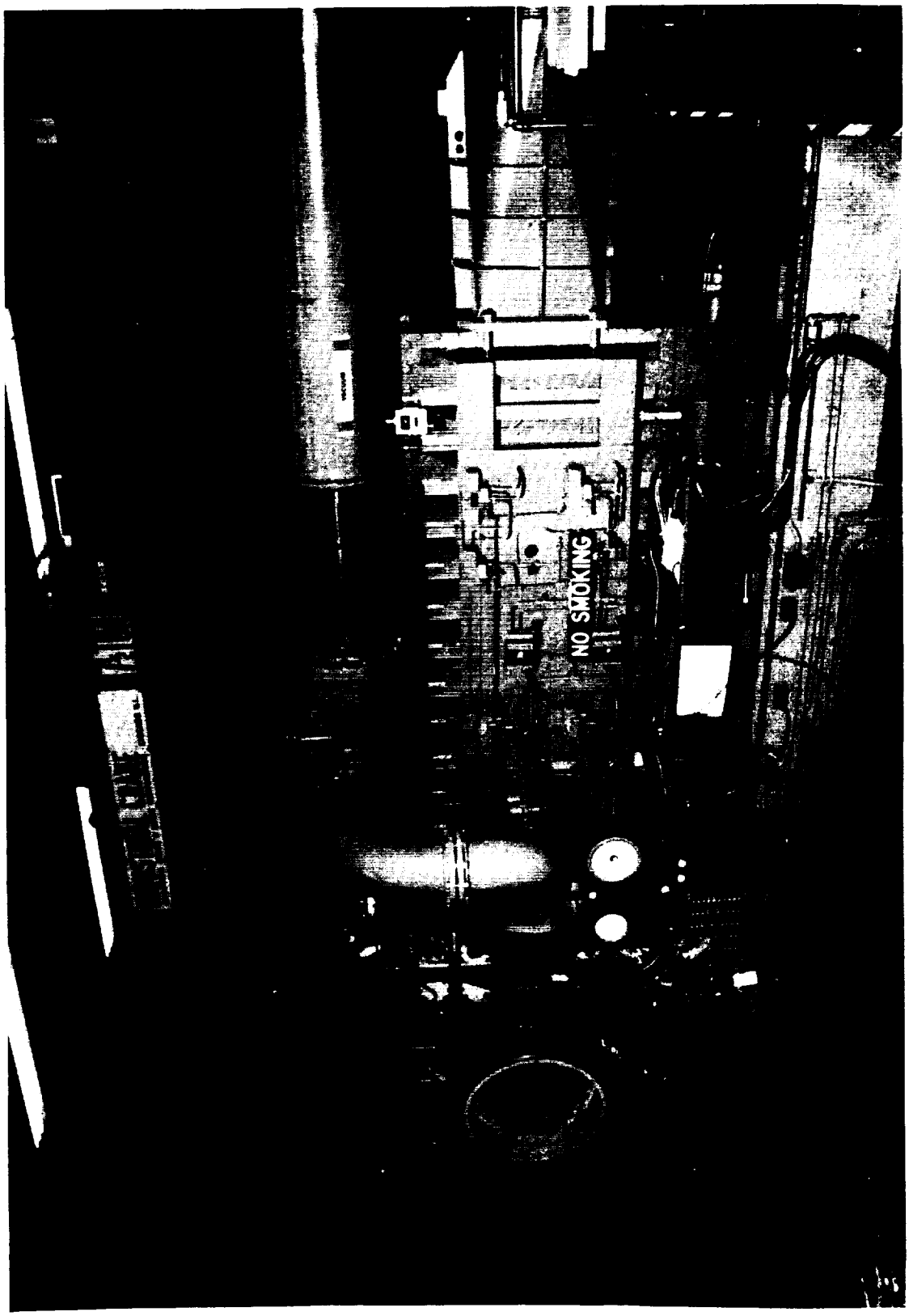

Figure 1. NASA MSFC's 14- by 14-in trisonic wind tunnel.

ORIGINAL PAGE
BLACK AND WHITE PHOTOGRAPH

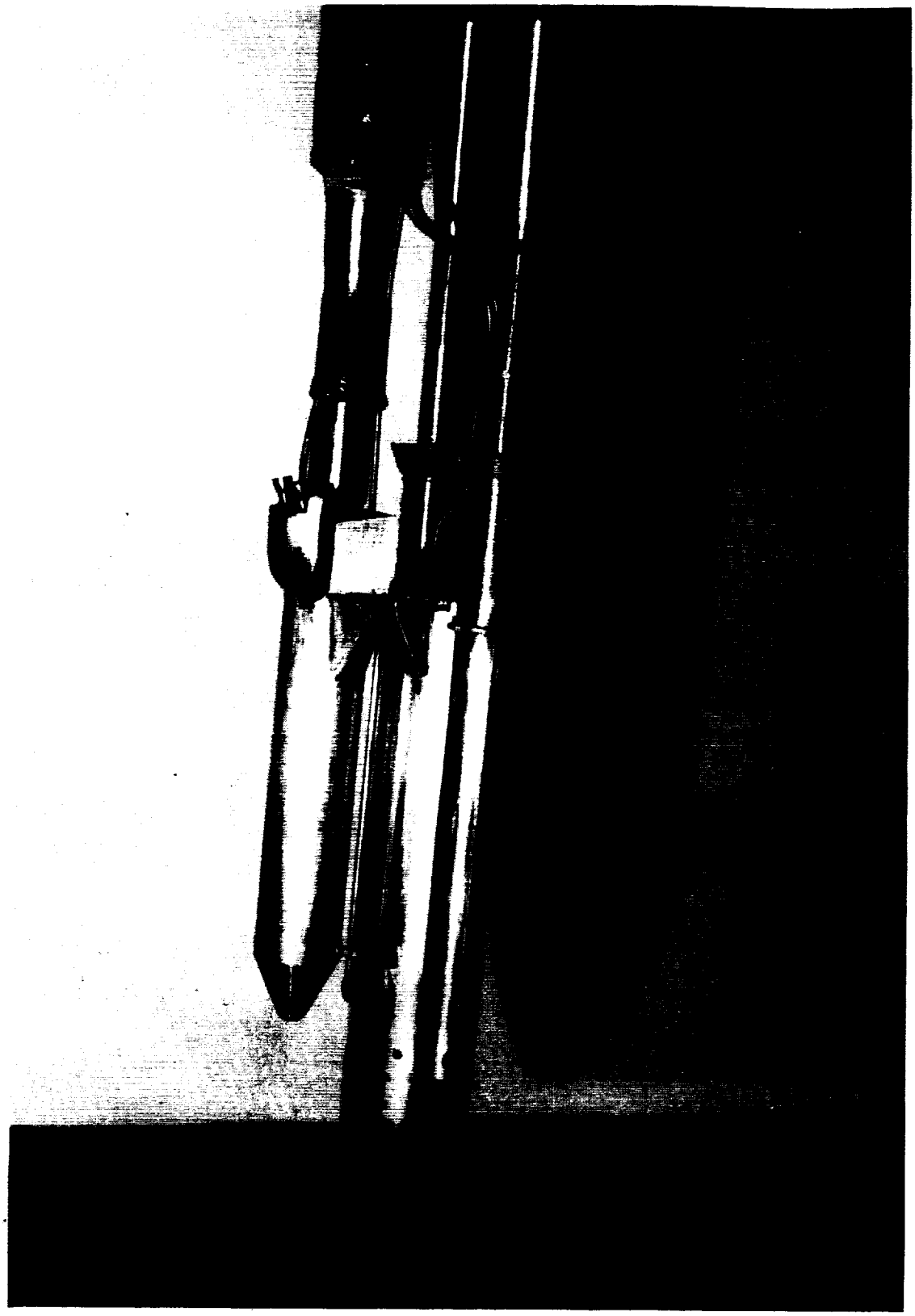

Figure 2. Shuttle-C reference configuration installed in the MSFC 14-in wind tunnel (TWT 715).

All dimensions in Inches

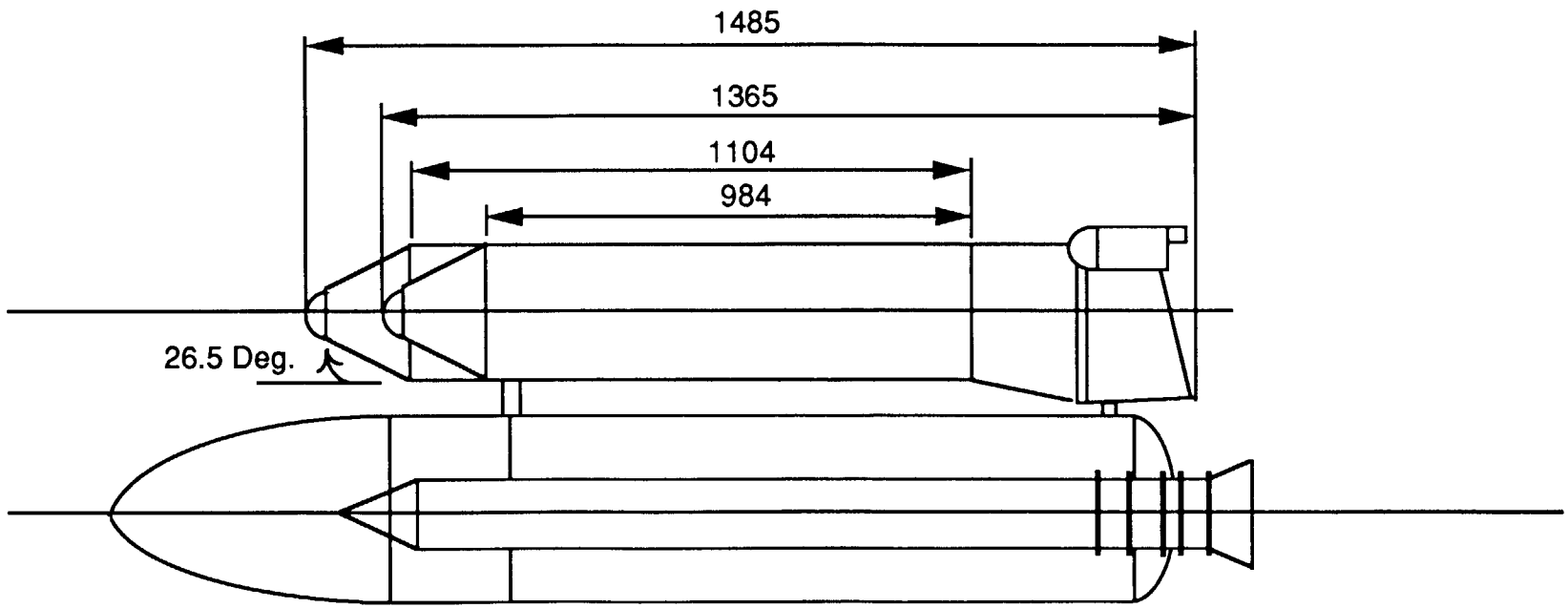

Figure 3. Shuttle-C cargo carrier configurations mated to lower stack.

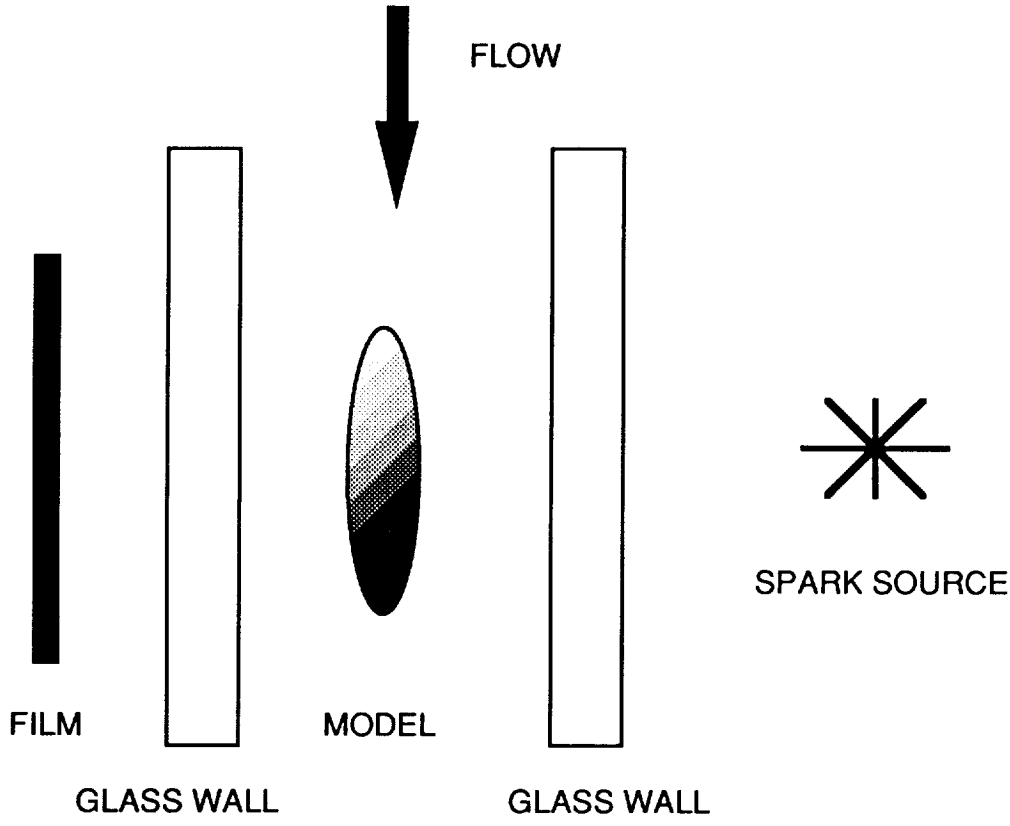

Figure 4. Sketch of shadowgraph setup.

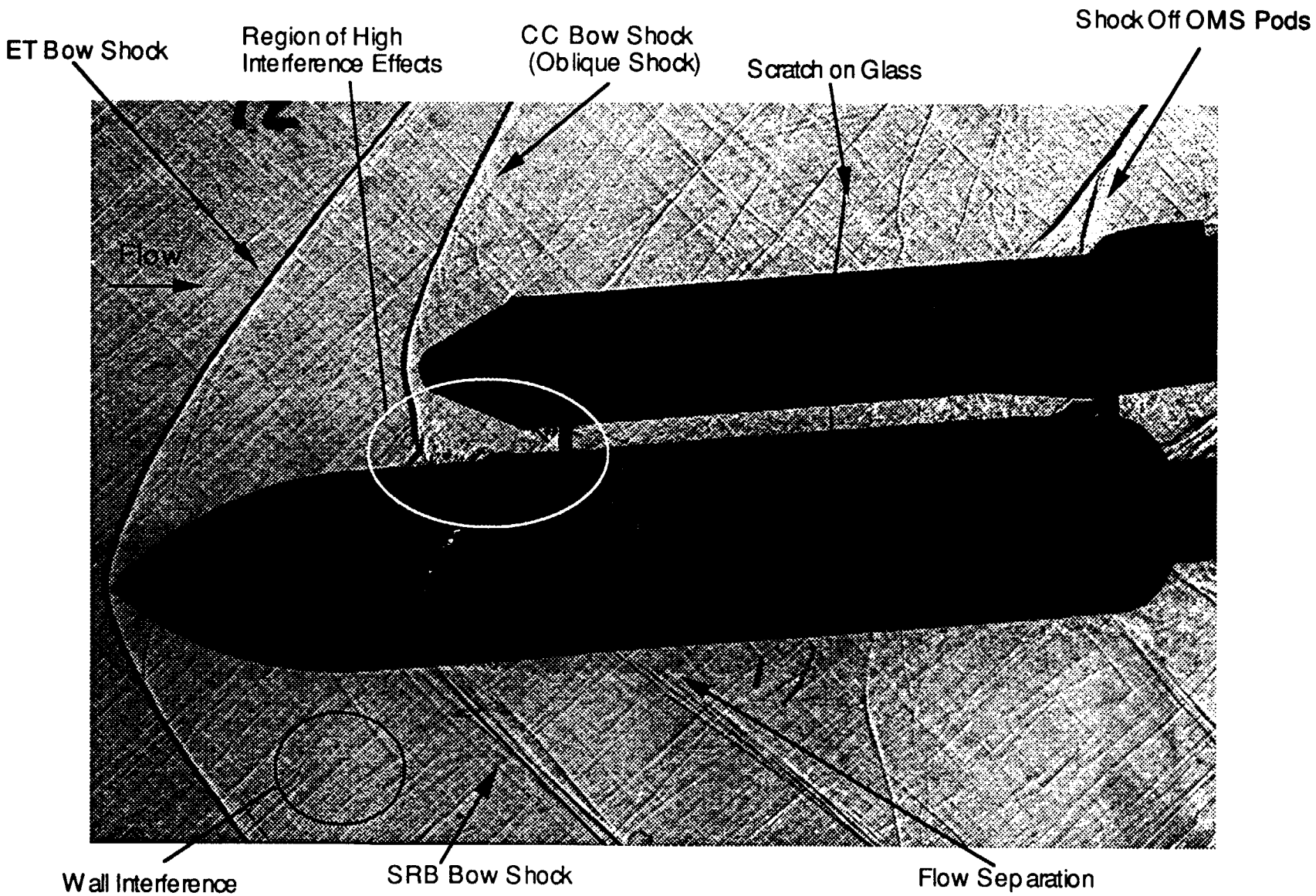

Figure 5. Reference configuration Mach 1.46, alpha = –4, beta = 0.

SECTION I

Reference Configuration
Alpha = 0, Beta = 0
Alpha = –4, Beta = 0
Roll Angle = 0

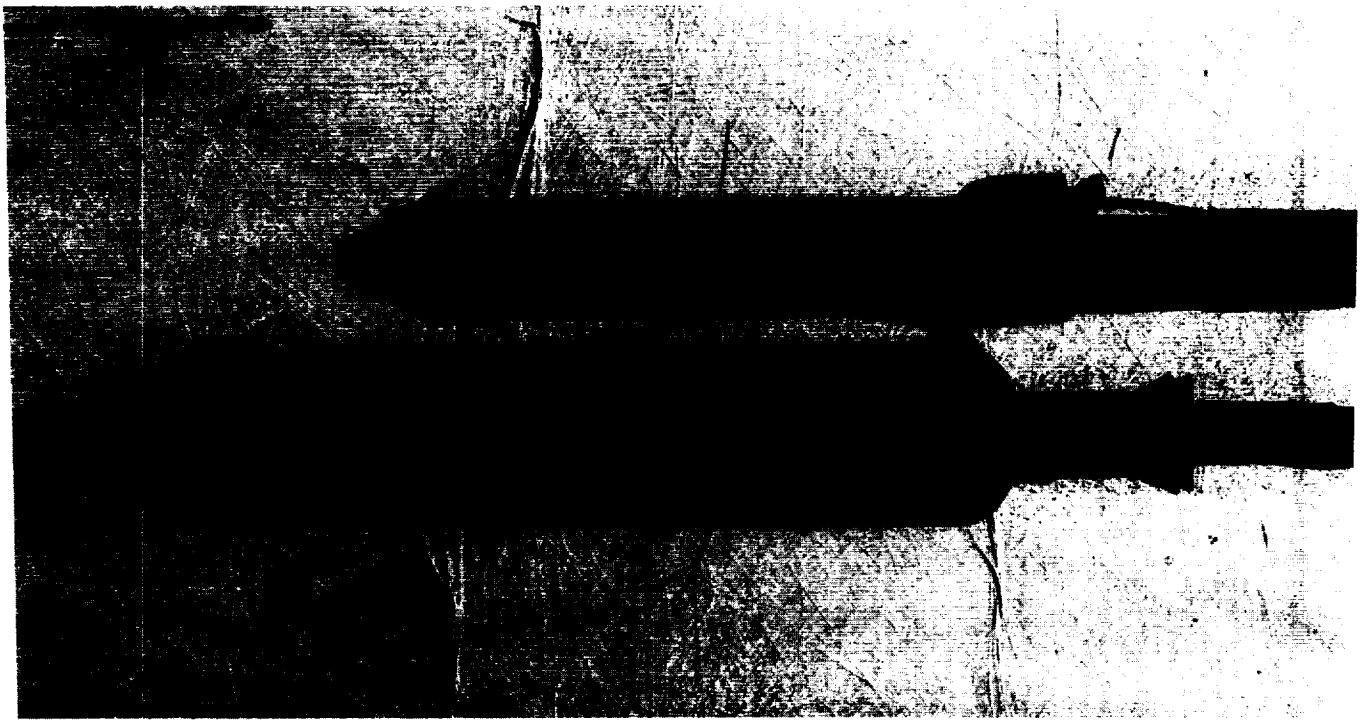

Figure 6. Reference configuration Mach 0.90, alpha = 0, beta = 0.

Figure 7. Reference configuration Mach 0.90, alpha = –4, beta = 0.

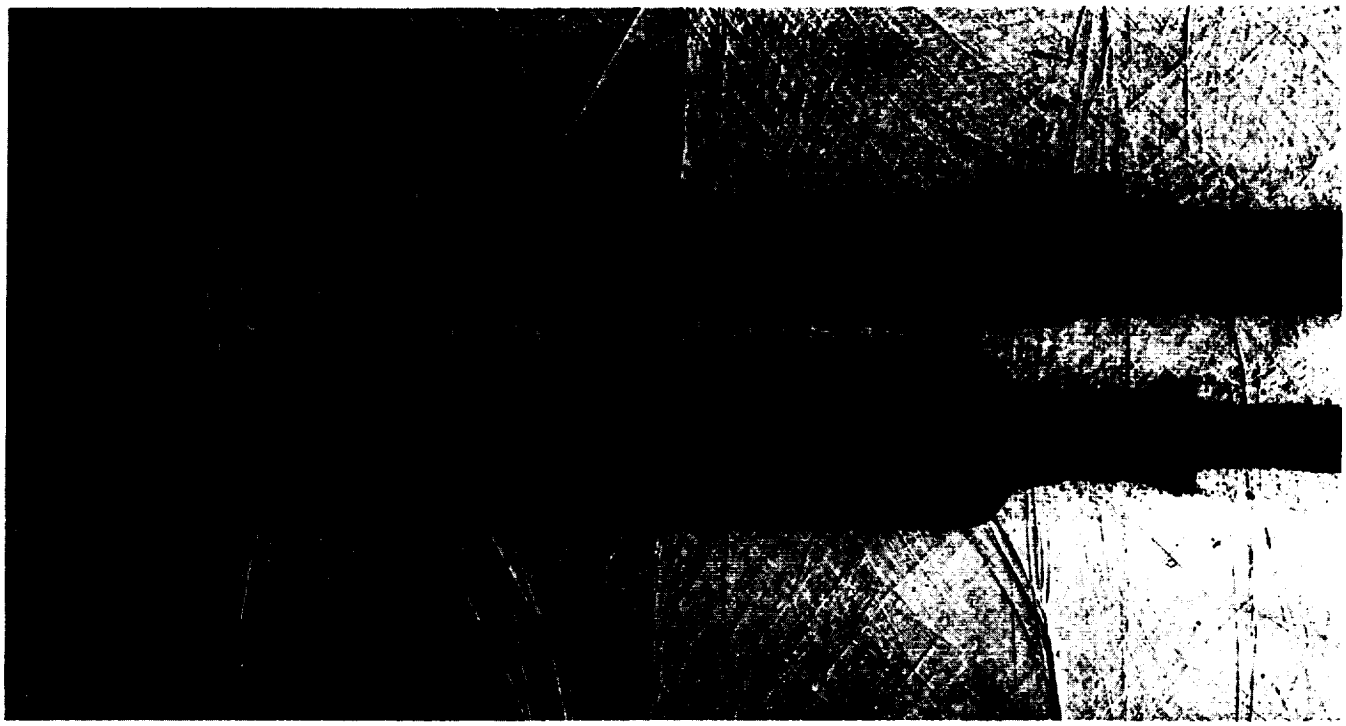

Figure 8. Reference configuration Mach 0.95, alpha = 0, beta = 0.

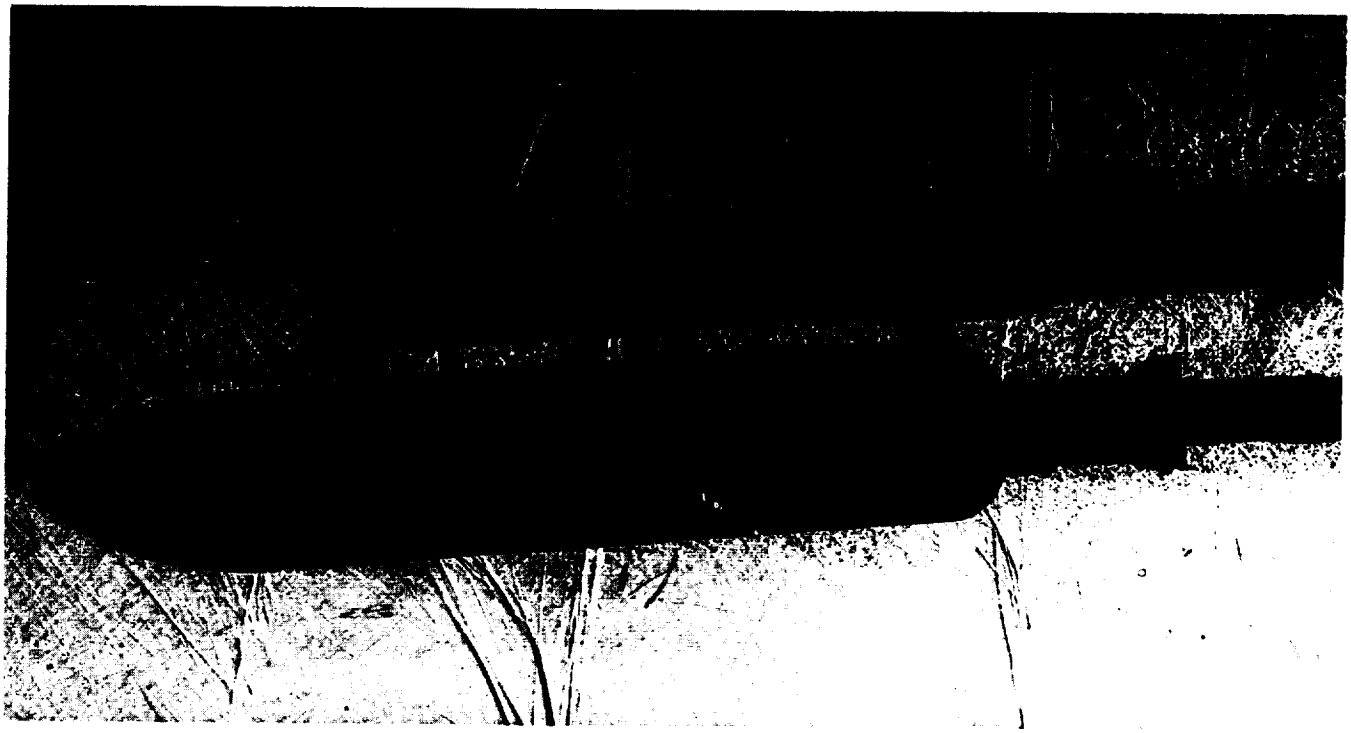

Figure 9. Reference configuration Mach 0.95, alpha = –4, beta = 0.

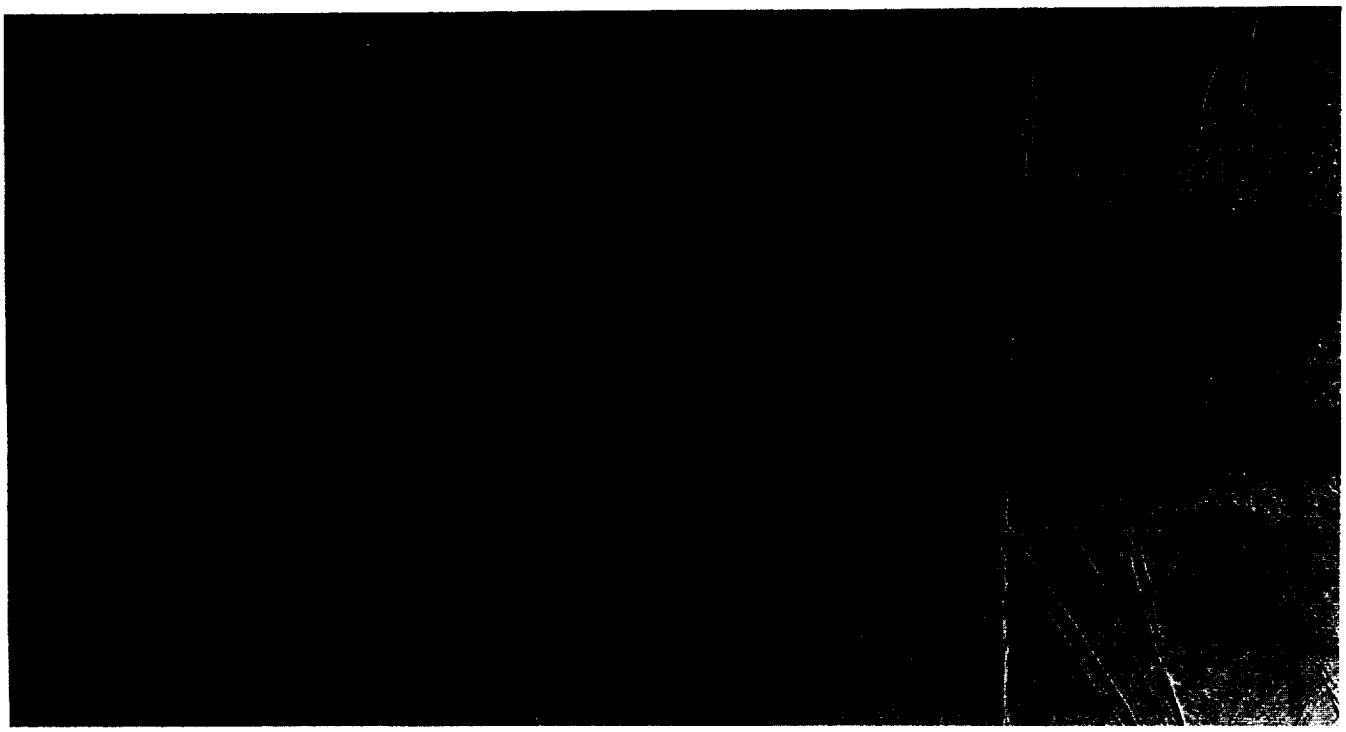

Figure 10. Reference configuration Mach 1.05, alpha = 0, beta = 0.

Figure 11. Reference configuration Mach 1.05, alpha = –4, beta = 0.

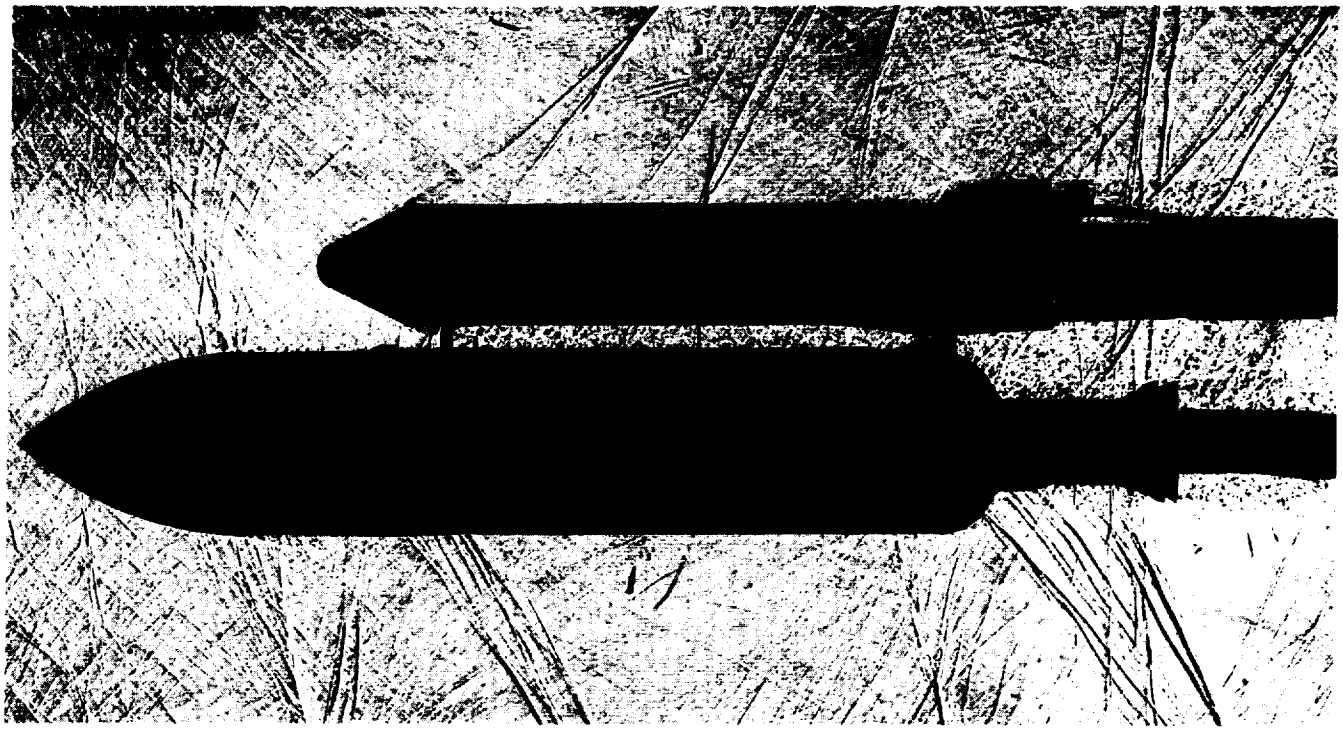

Figure 12. Reference configuration Mach 1.10, alpha = 0, beta = 0.

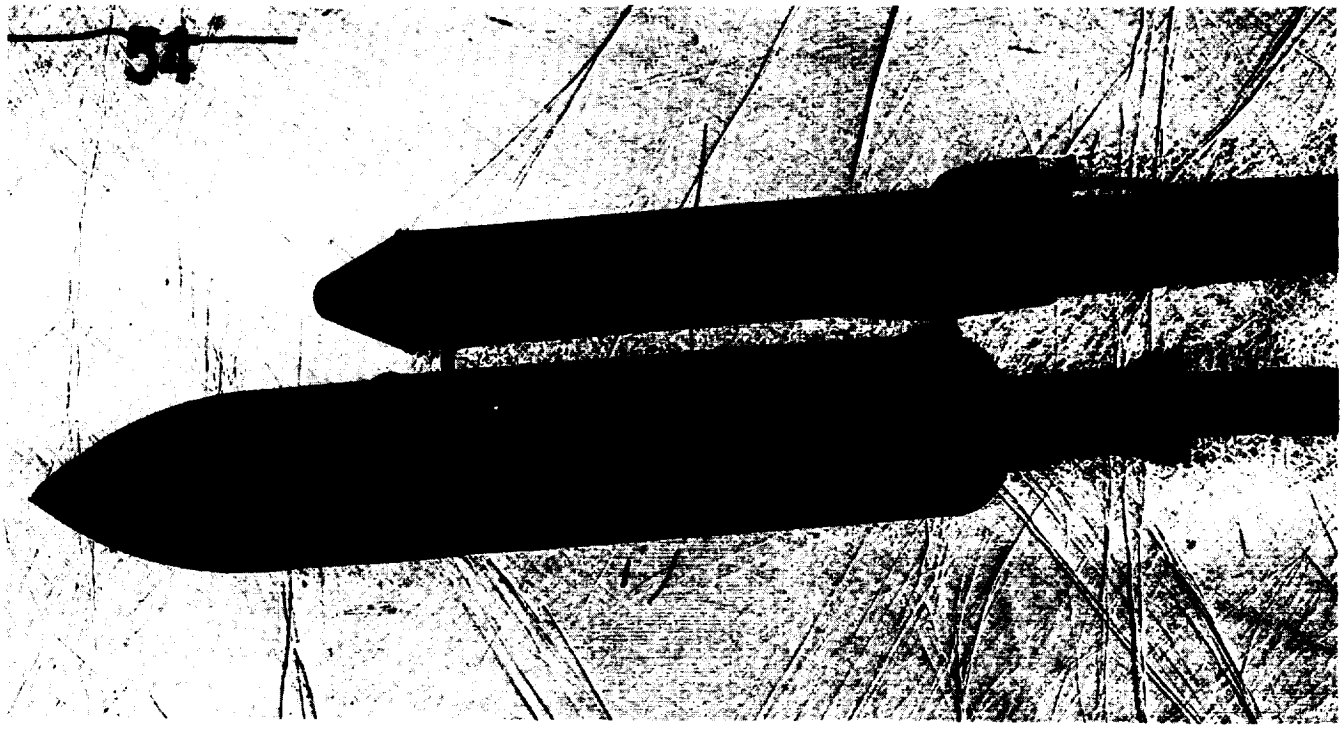

Figure 13. Reference configuration Mach 1.10, alpha = –4, beta = 0.

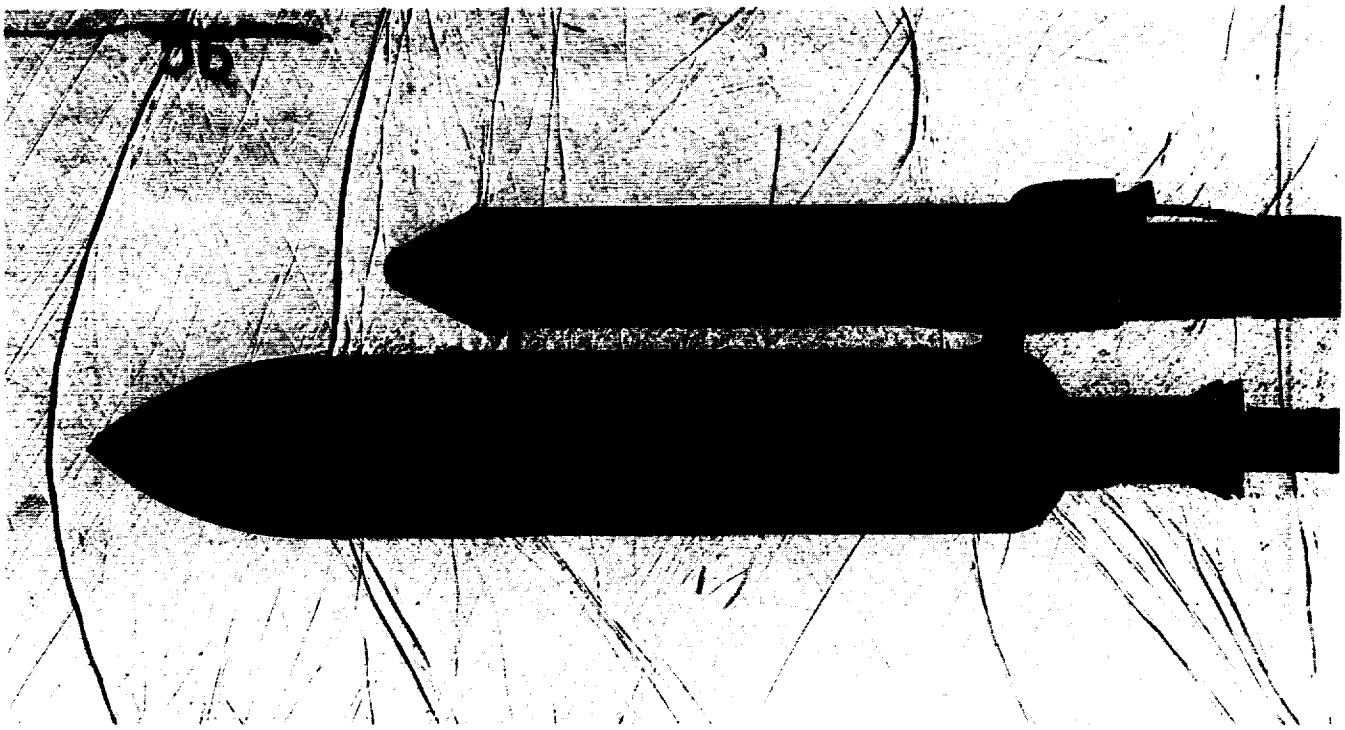

Figure 14. Reference configuration Mach 1.25, alpha = 0, beta = 0

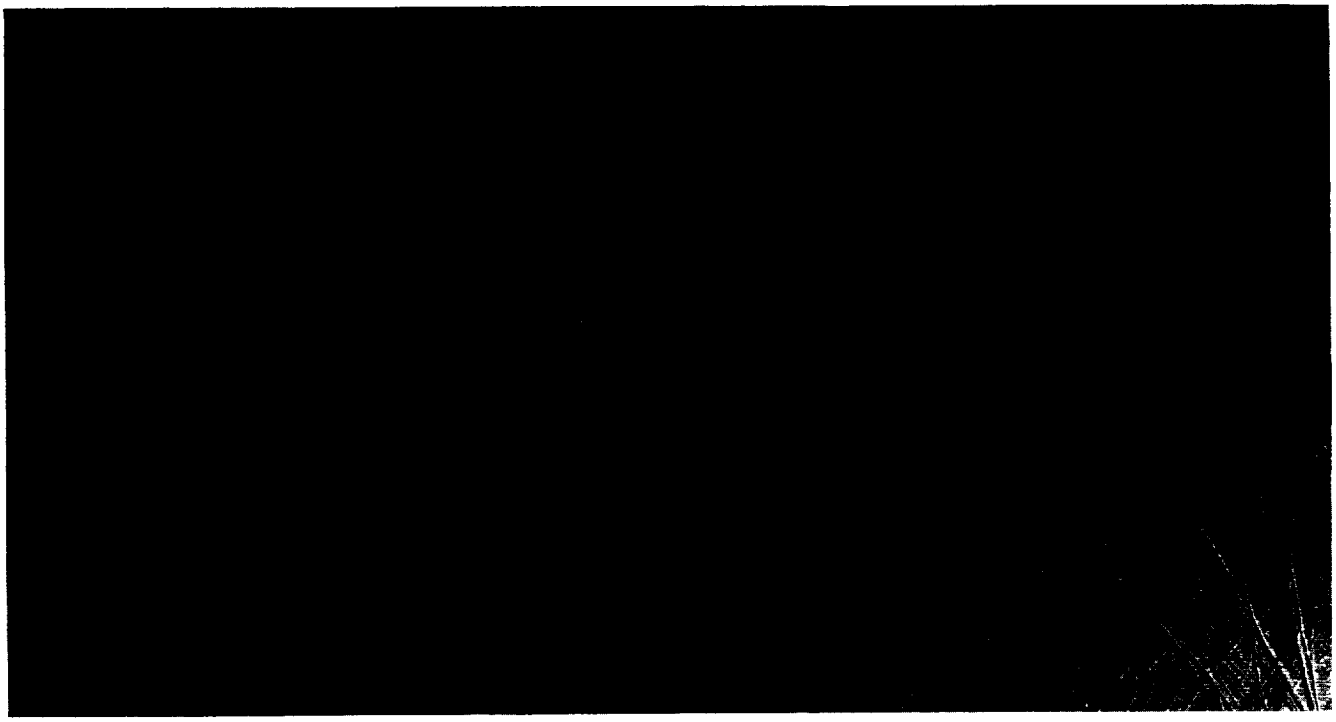

Figure 15. Reference configuration Mach 1.25, alpha = –4, beta = 0.

Figure 16. Reference configuration Mach 1.46, alpha = 0, beta = 0.

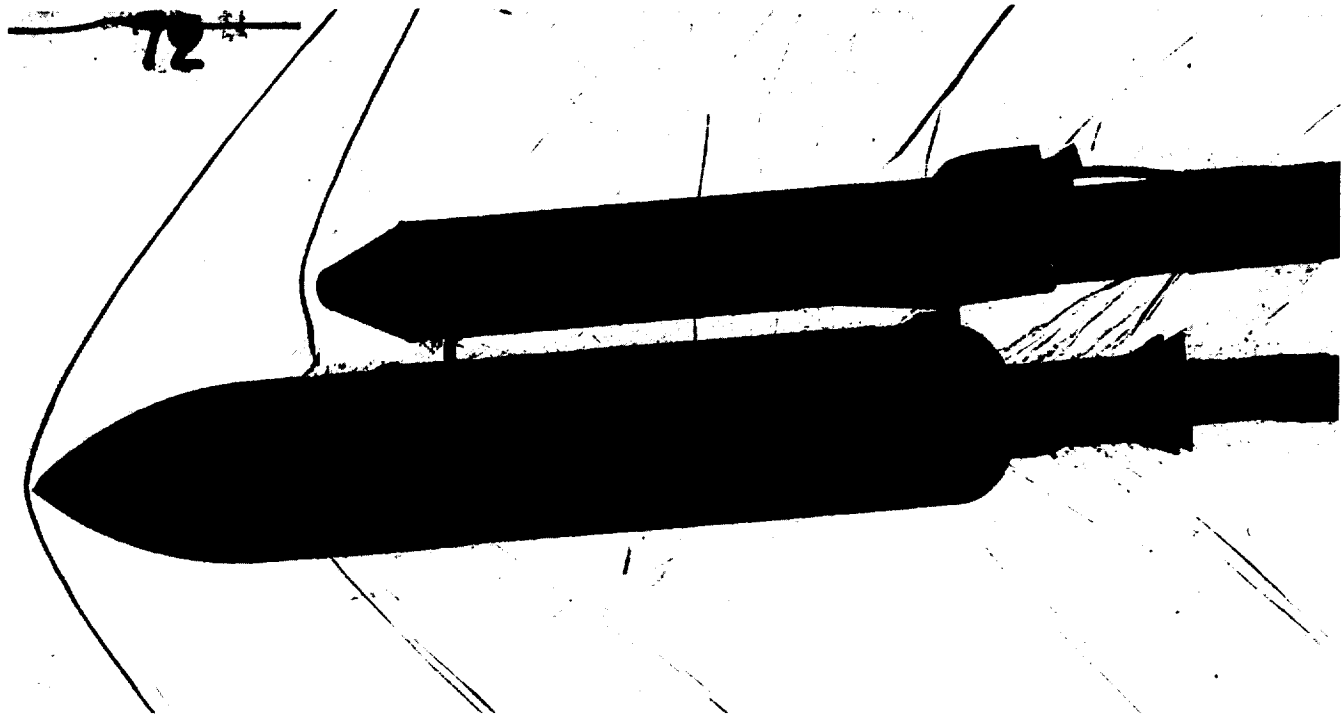

Figure 17. Reference configuration Mach 1.46, alpha = –4, beta = 0.

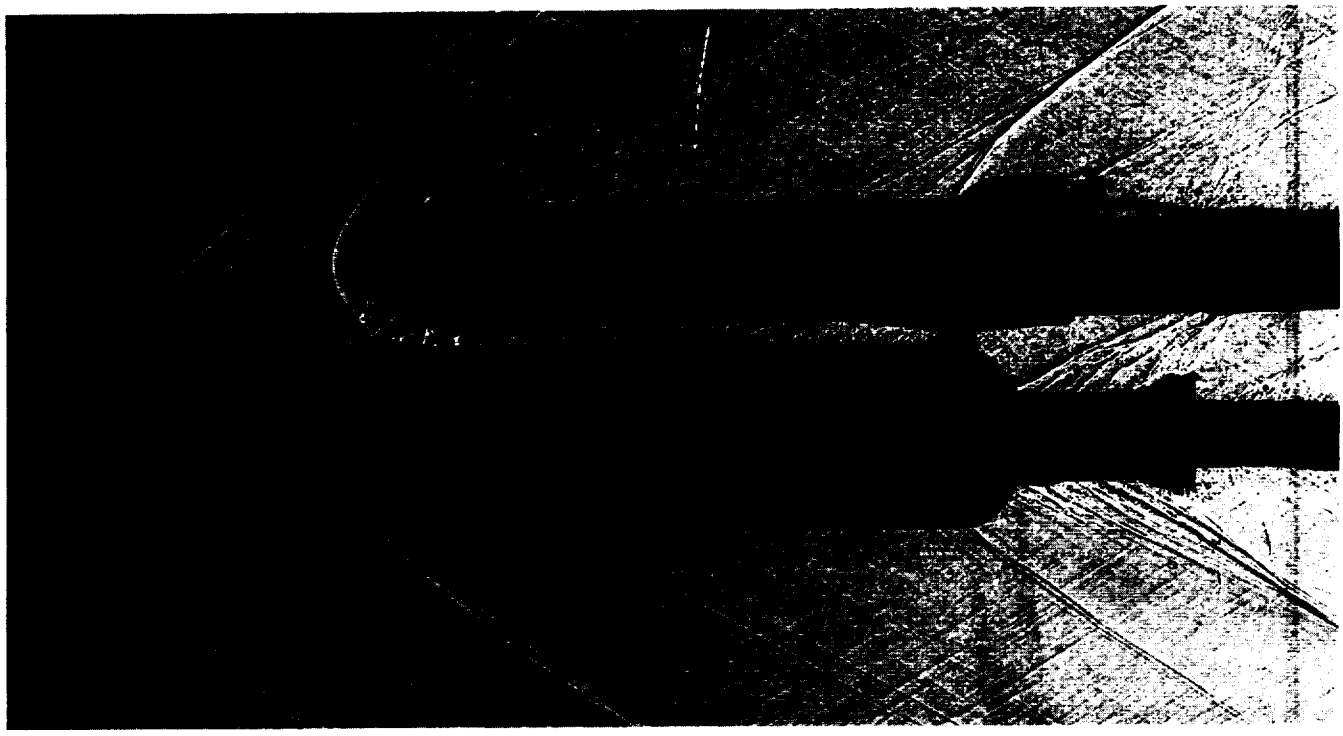

Figure 18. Reference configuration Mach 1.96, alpha = 0, beta = 0.

Figure 19. Reference configuration Mach 1.96, alpha = –4, beta = 0.

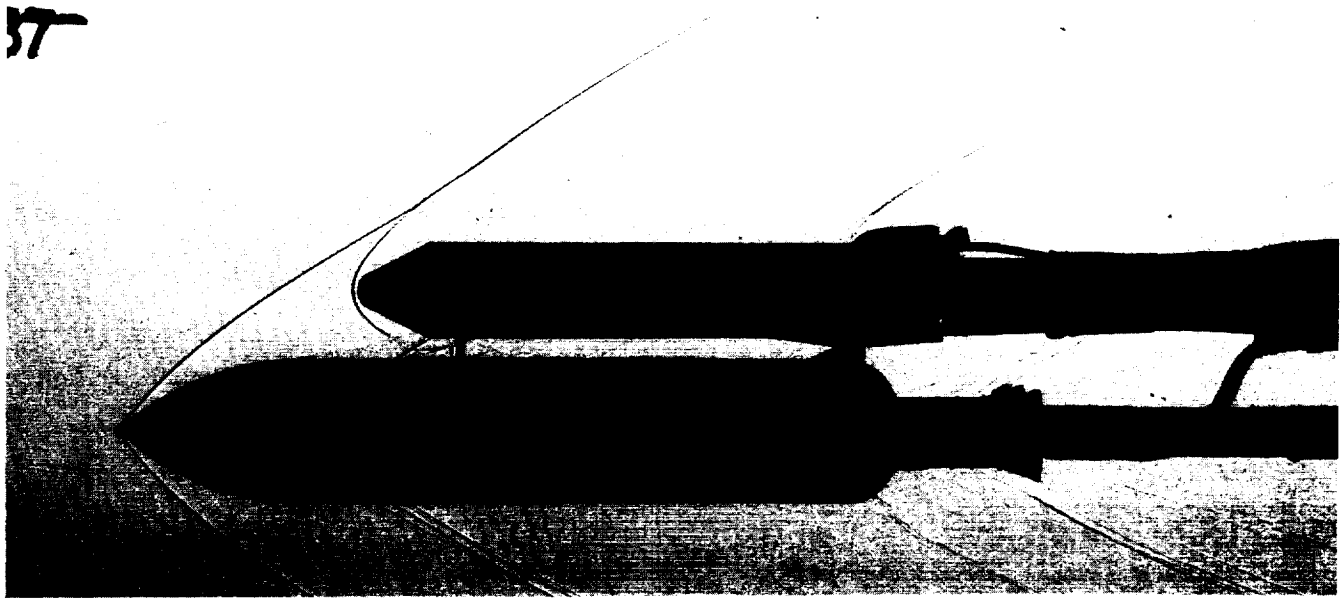

Figure 20. Reference configuration Mach 2.74, alpha = 0, beta = 0.

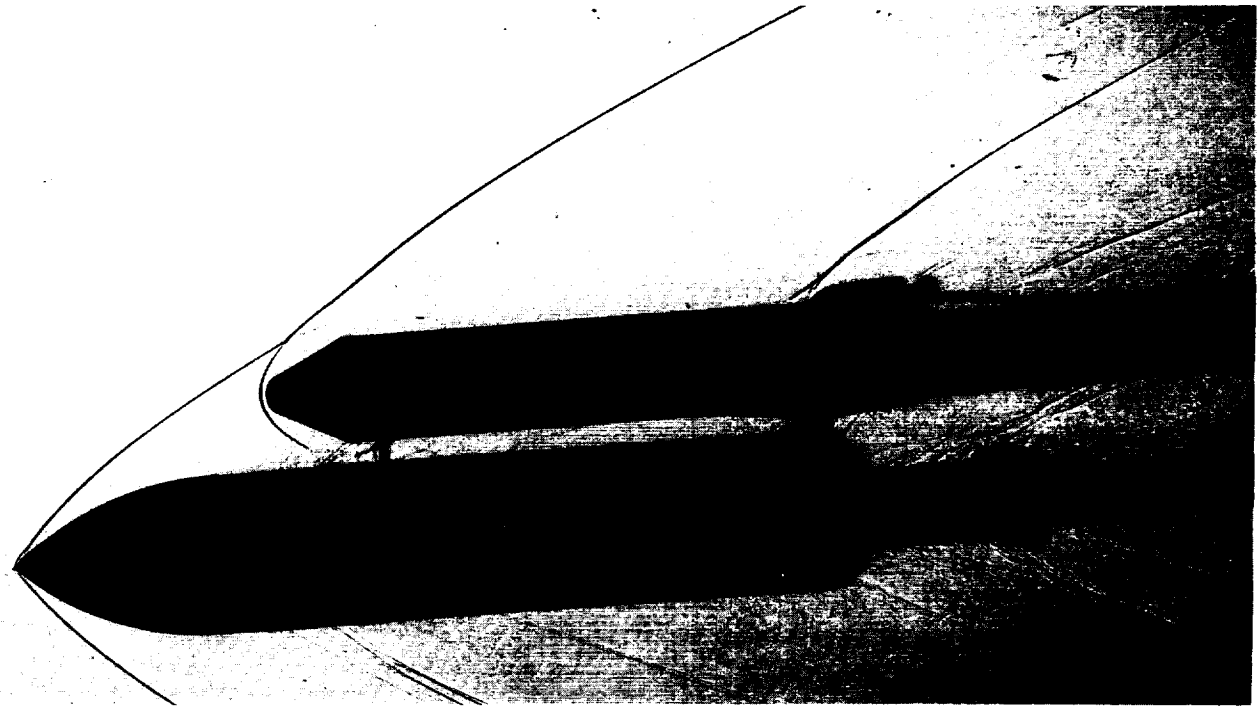

Figure 21. Reference configuration Mach 2.74, alpha = –4, beta = 0.

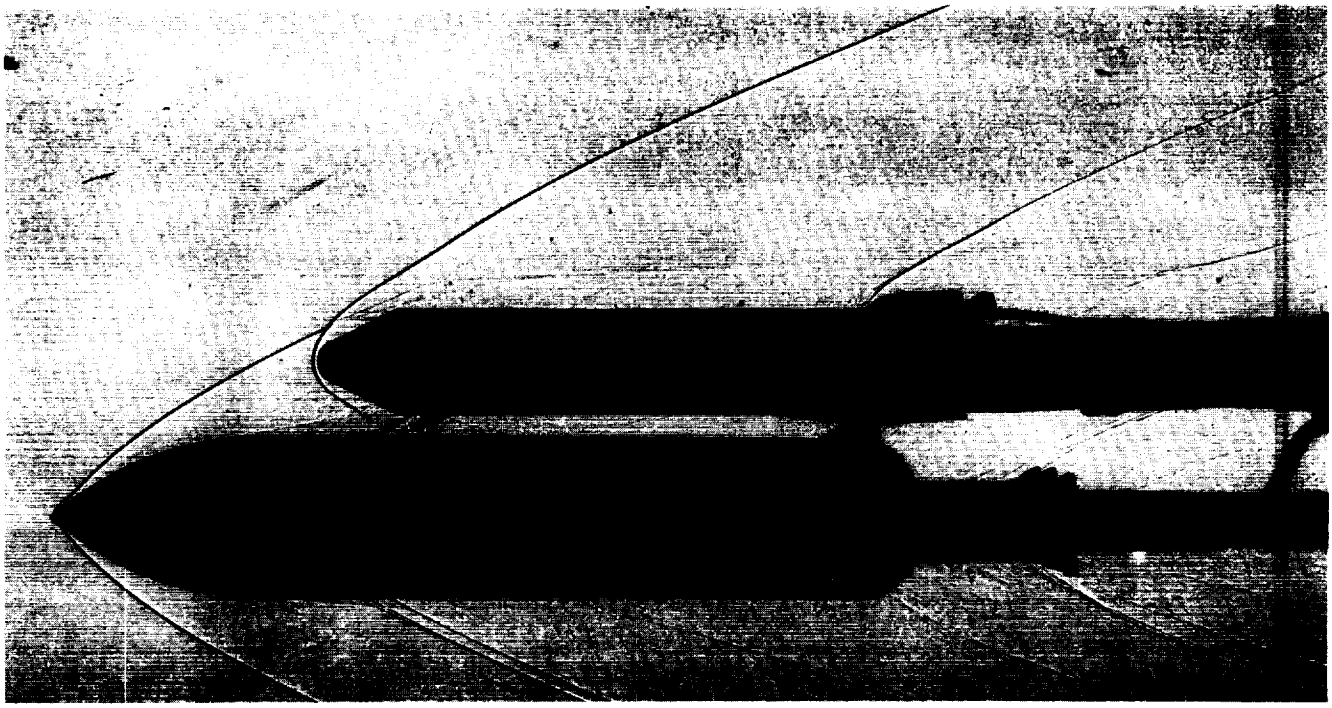

Figure 22. Reference configuration Mach 3.48, alpha = 0, beta = 0.

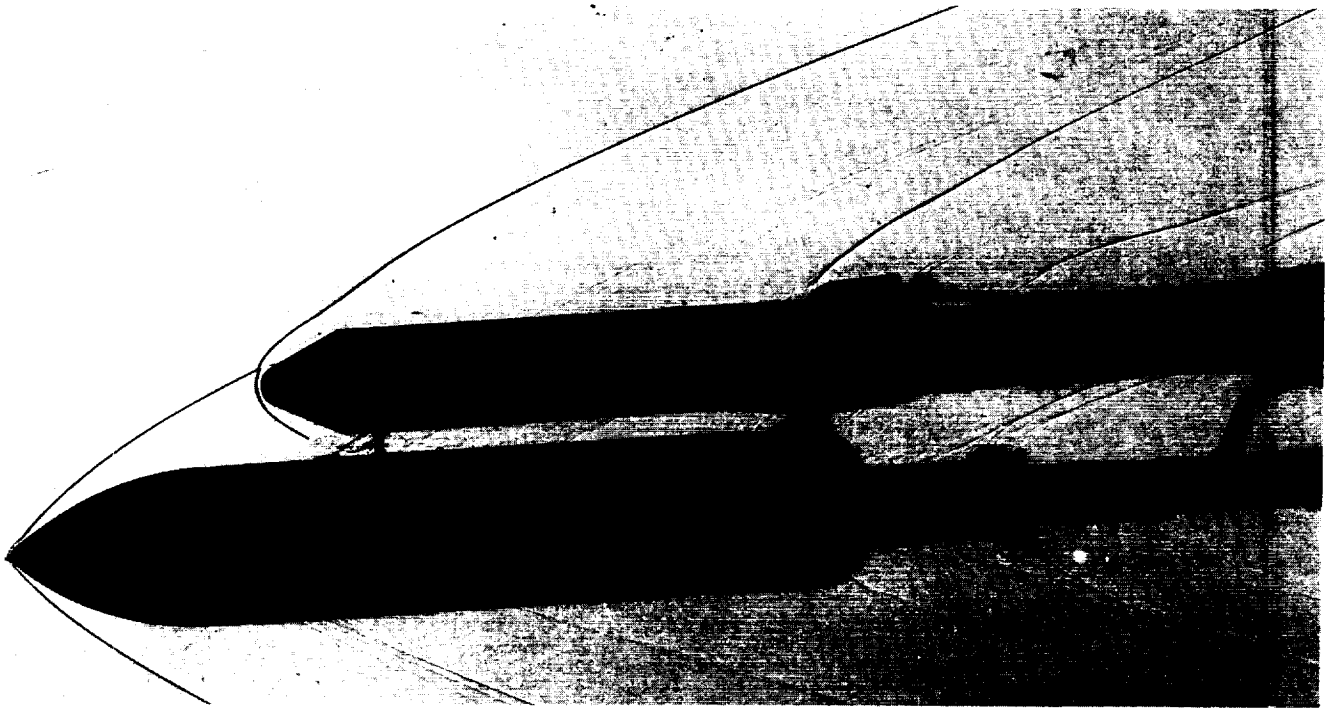

Figure 23. Reference configuration Mach 3.48, alpha = –4, beta = 0.

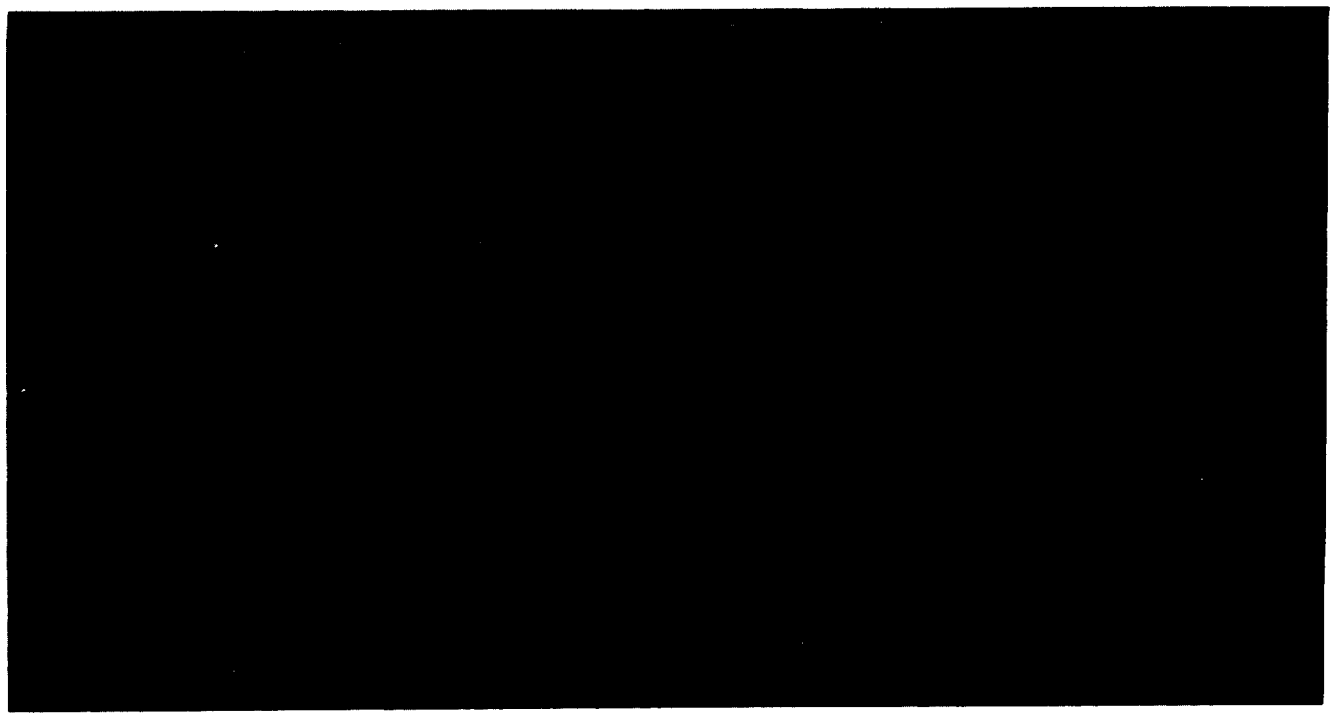

Figure 24. Reference configuration Mach 4.95, alpha = 0, beta = 0.

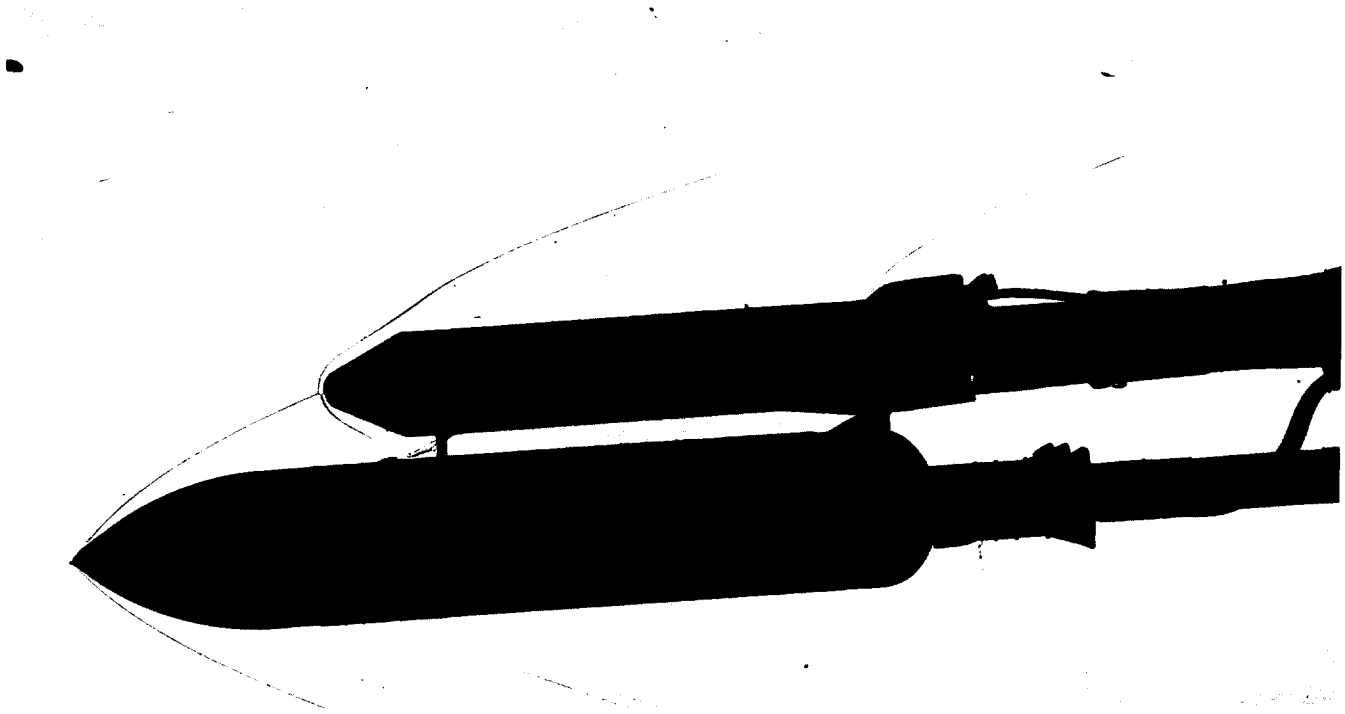

Figure 25. Reference configuration Mach 4.95, alpha = –4, beta = 0.

SECTION II

Reference Configuration
Alpha = 0, Beta = 0
Roll Angle = 90°

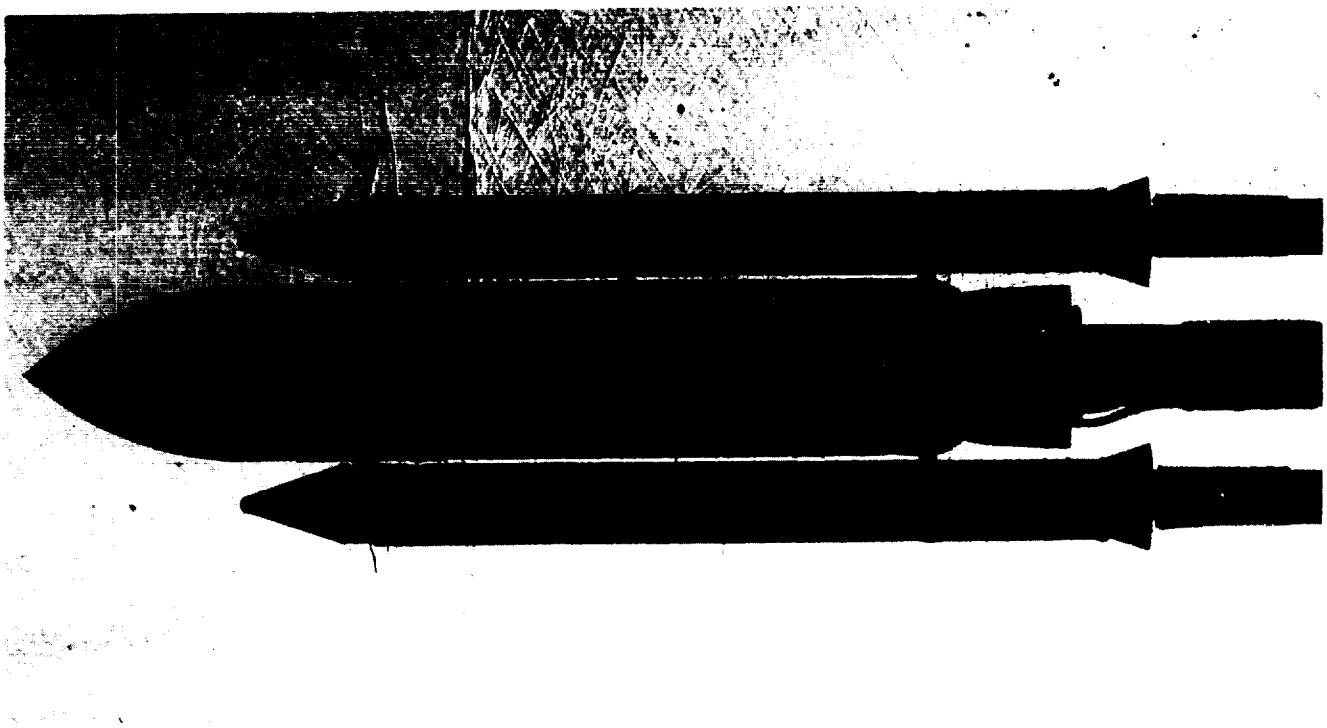

Figure 26. Reference configuration Mach 0.90, alpha = 0, beta = 0, roll = 90°.

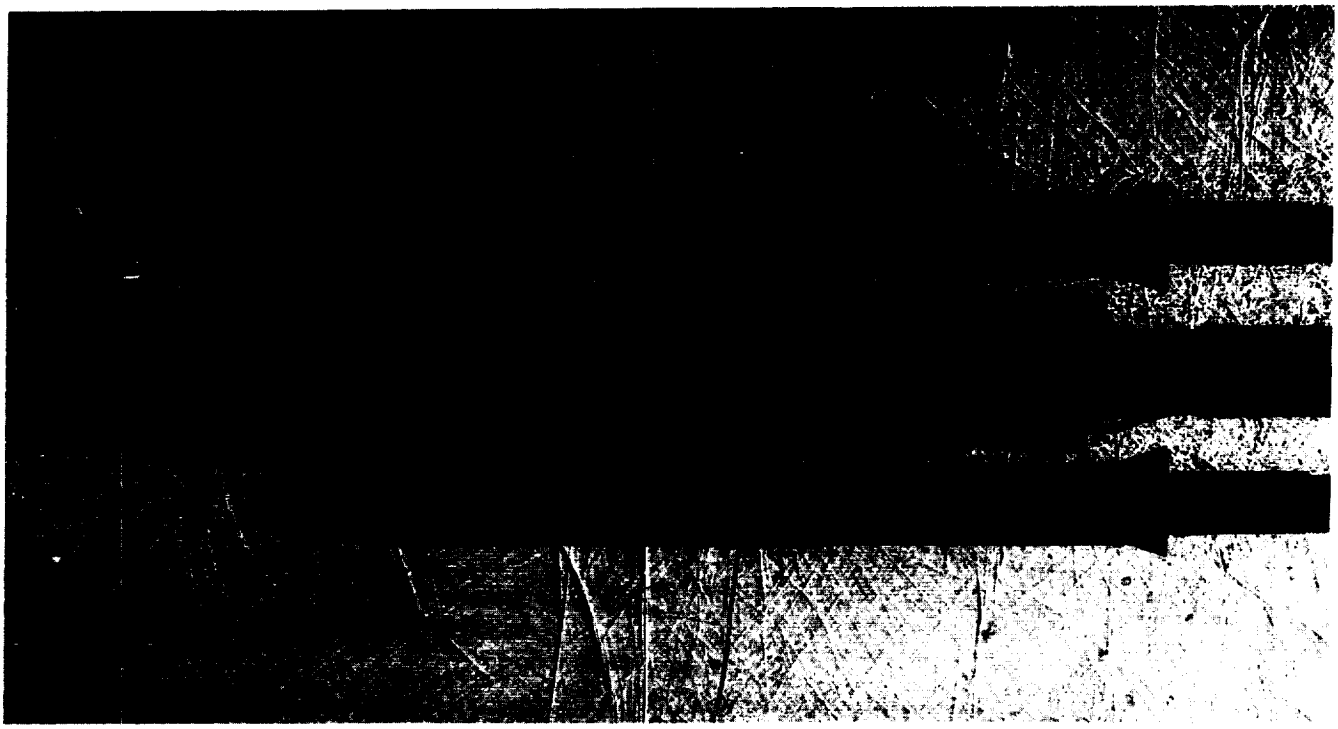

Figure 27. Reference configuration Mach 0.95, alpha = 0, beta = 0, roll = 90°.

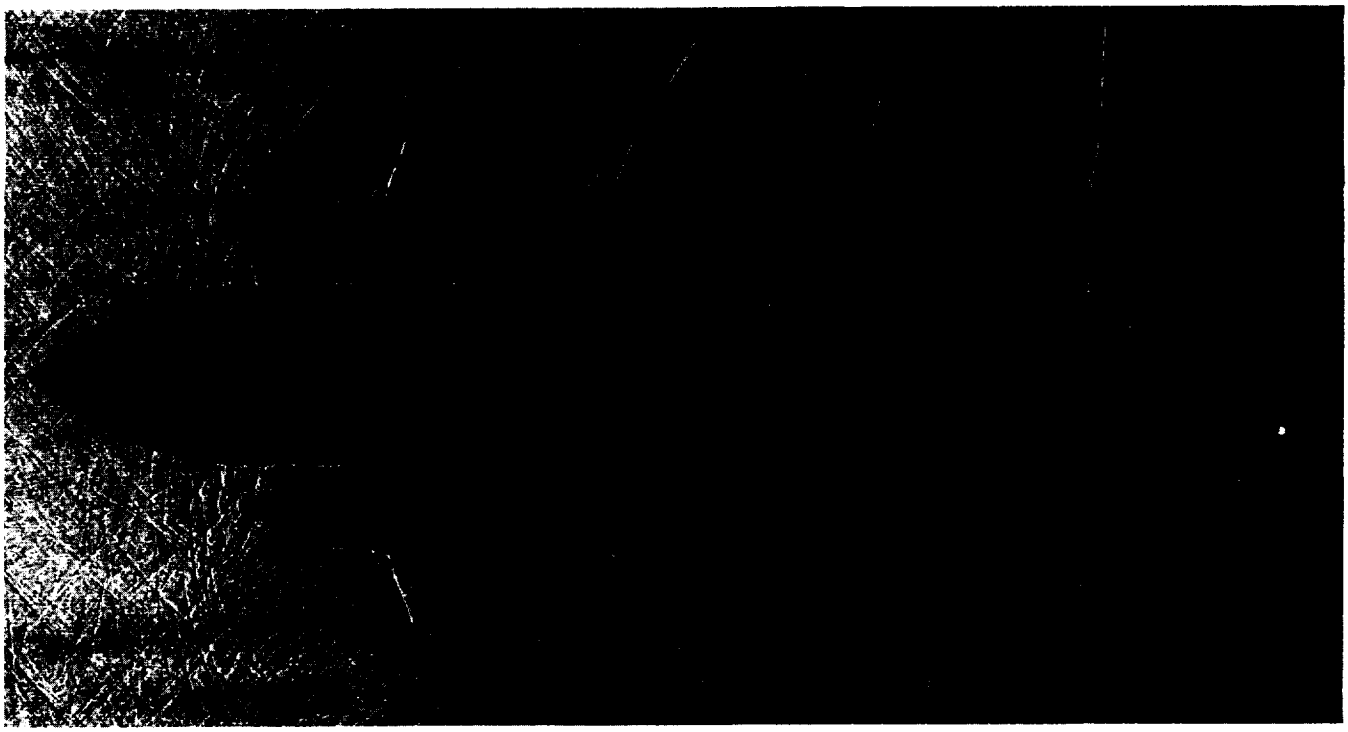

Figure 28. Reference configuration Mach 1.05, alpha = 0, beta = 0, roll = 90°.

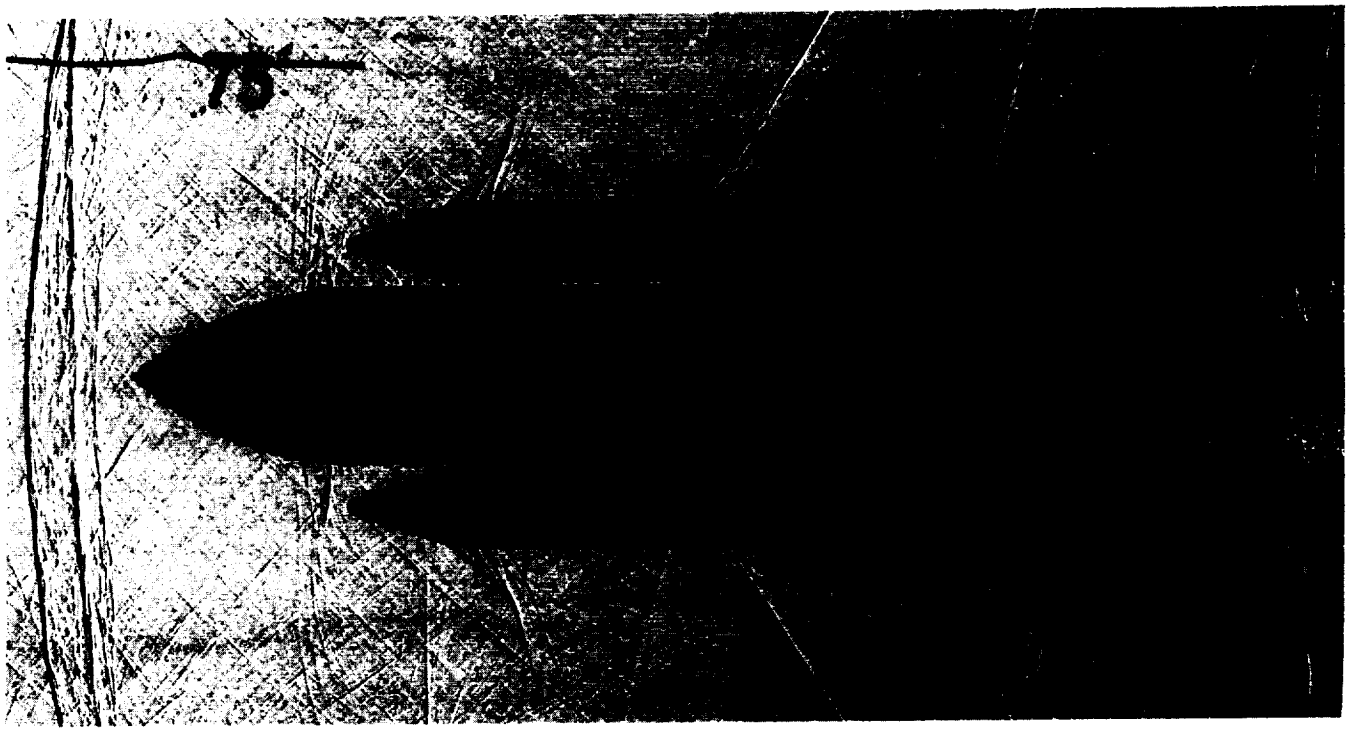

Figure 29. Reference configuration Mach 1.10, alpha = 0, beta = 0, roll = 90°.

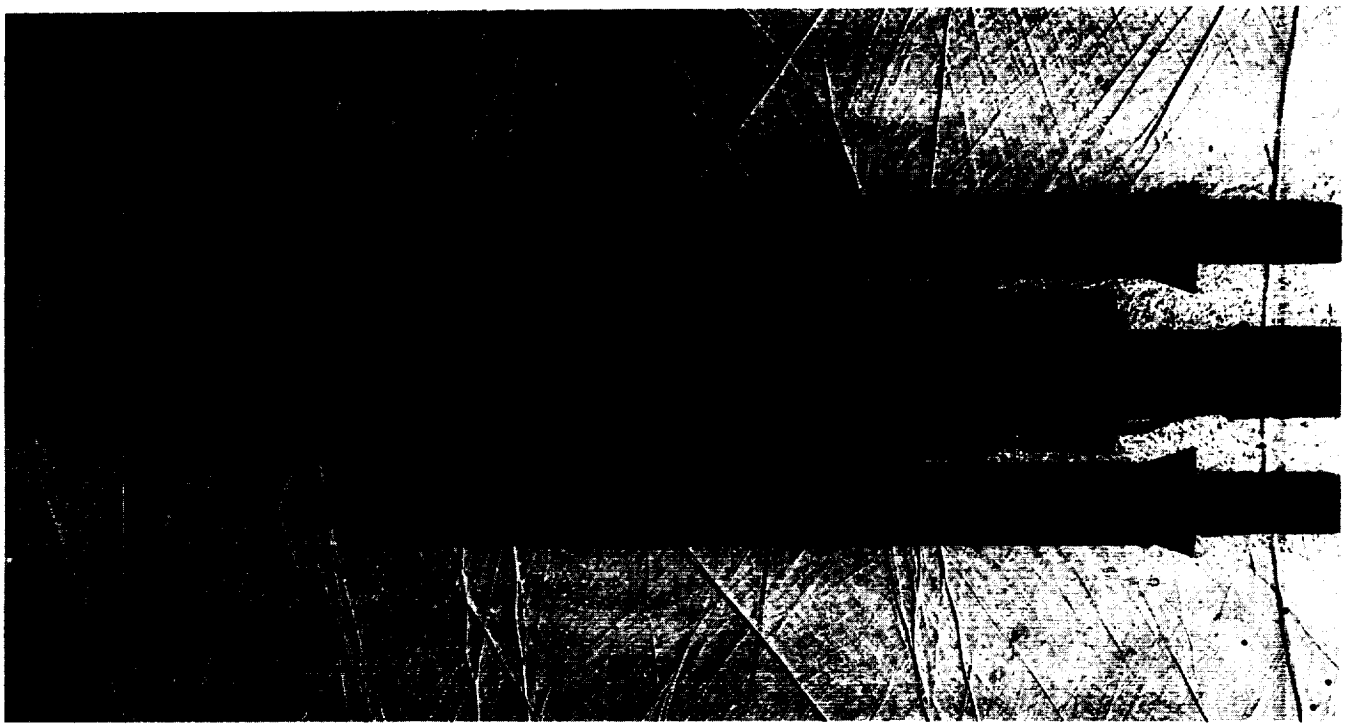

Figure 30. Reference configuration Mach 1.25, alpha = 0, beta = 0, roll = 90°.

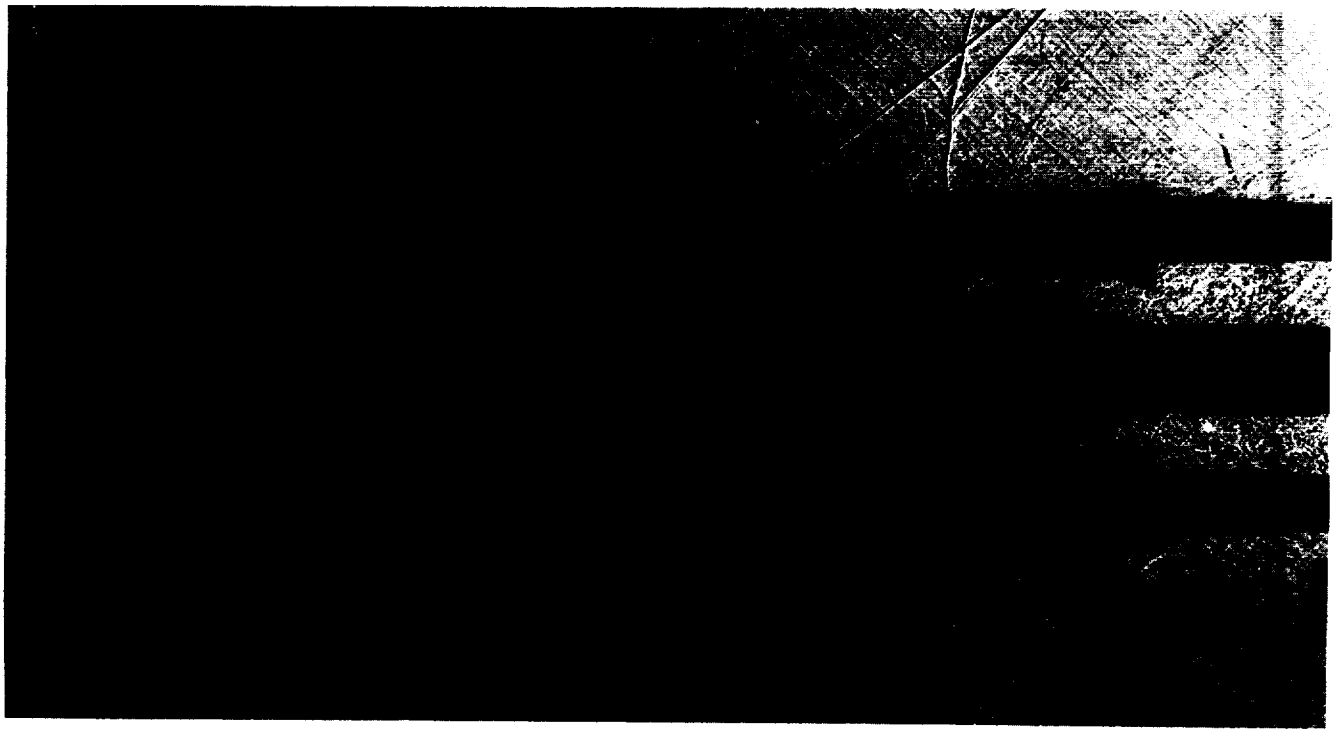

Figure 31. Reference configuration Mach 1.46, alpha = 0, beta = 0, roll = 90°.

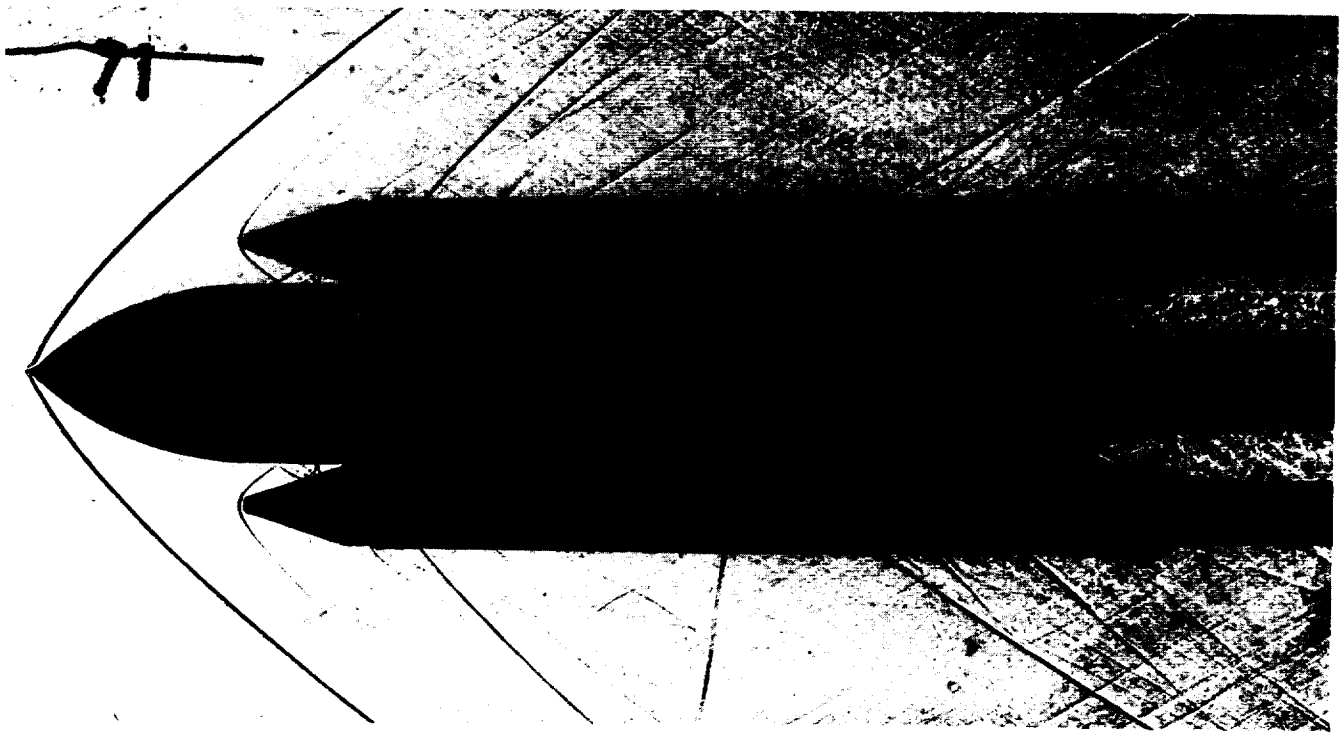

Figure 32. Reference configuration Mach 1.96, alpha = 0, beta = 0, roll = 90°.

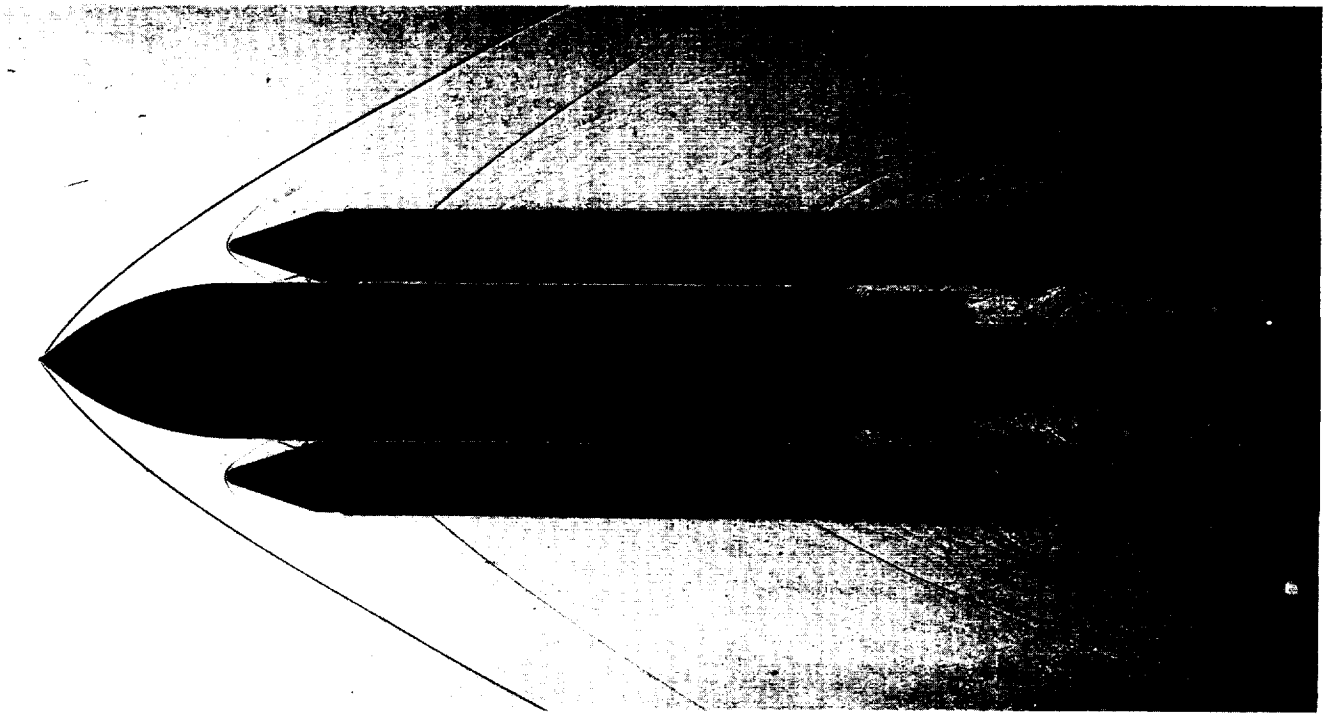

Figure 33. Reference configuration Mach 2.74, alpha = 0, beta = 0, roll = 90°.

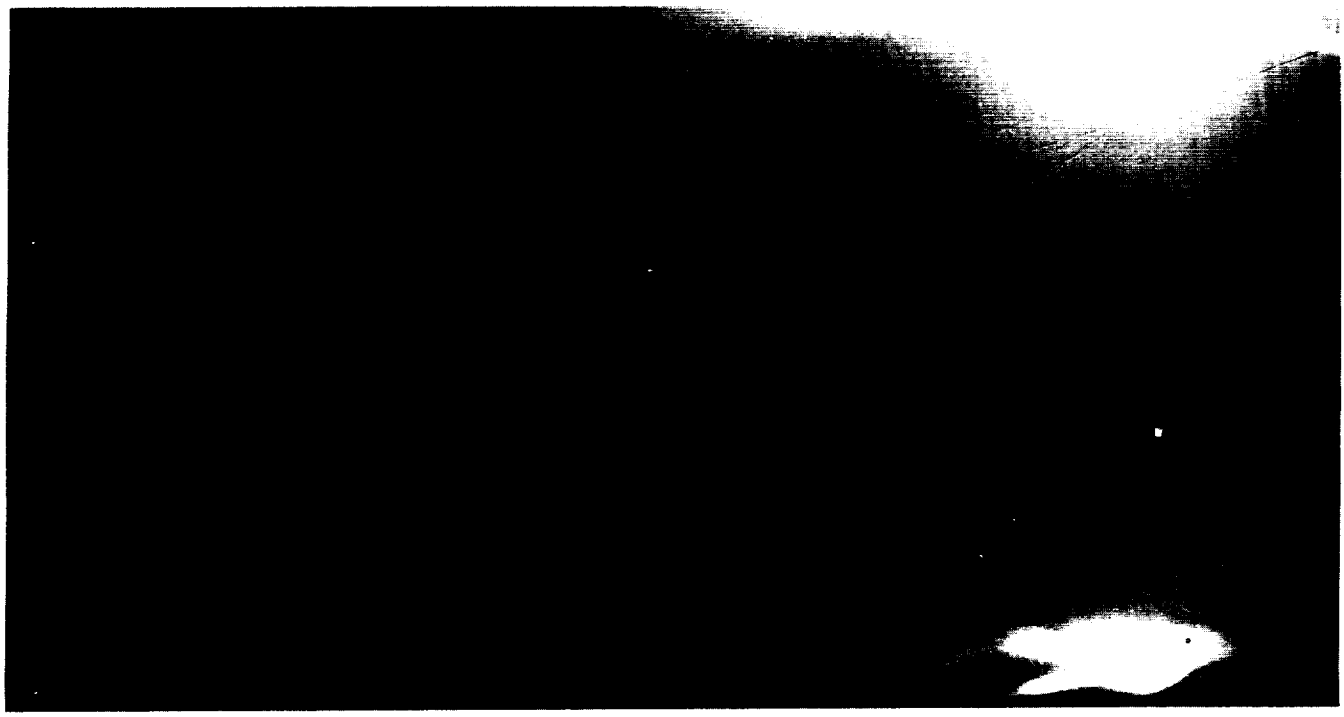

Figure 34. Reference configuration Mach 3.48, alpha = 0, beta = 0, roll = 90°.

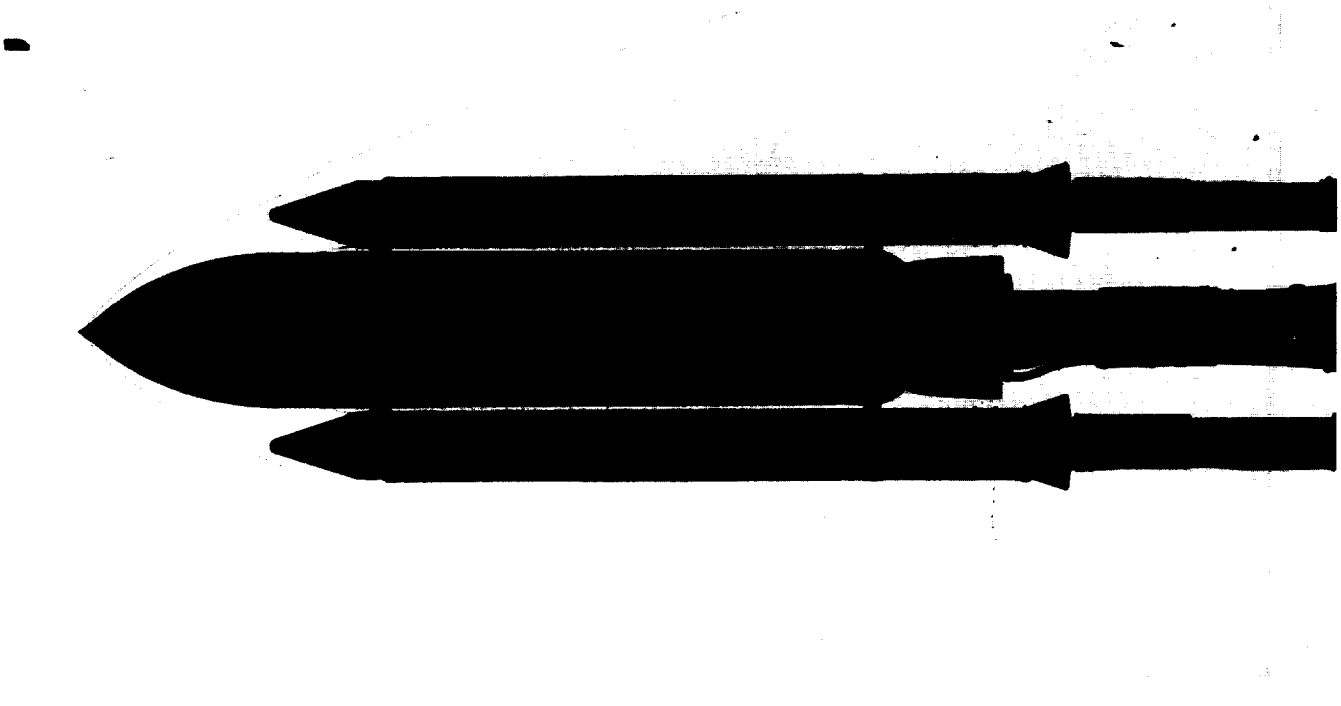

Figure 35. Reference configuration Mach 4.95, alpha = 0, beta = 0, roll = 90°.

SECTION III

CYL-92-26-MV Configuration
Alpha = 0, Beta = 0
Alpha = –4, Beta = 0
Roll = 0

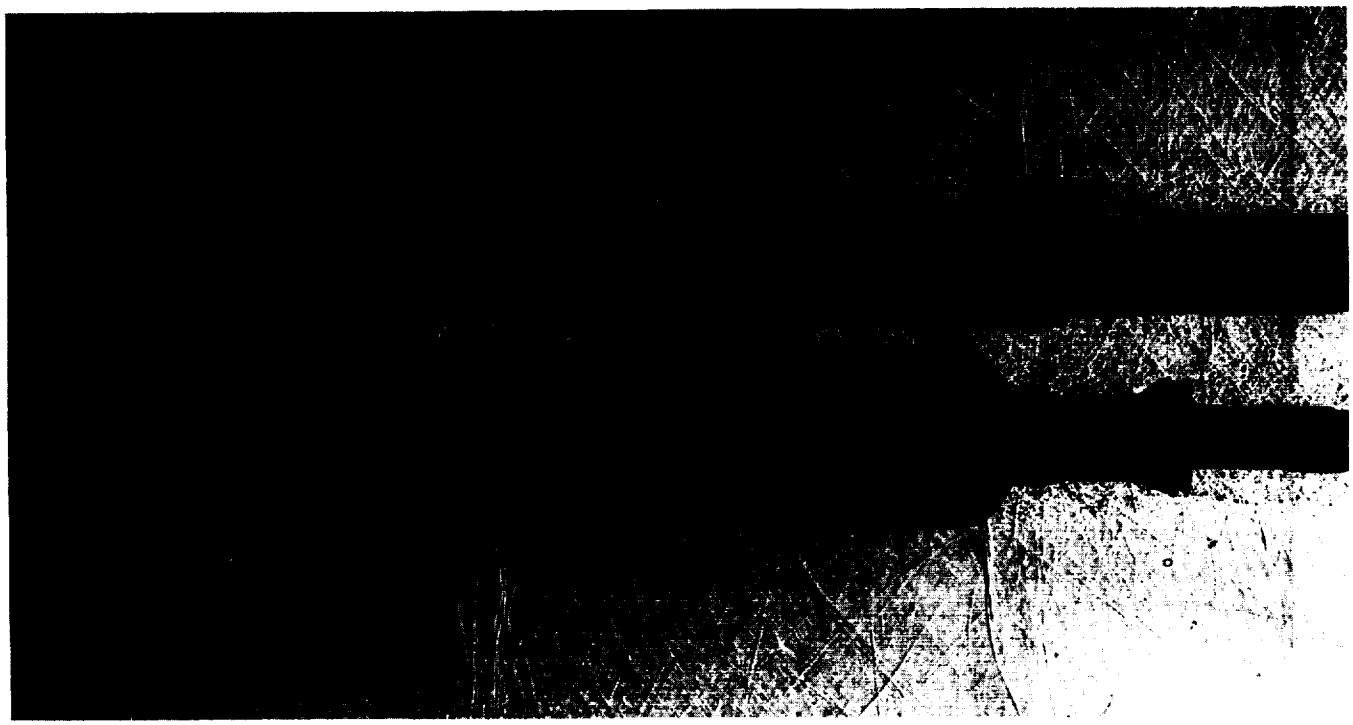

Figure 36. CYL-92-26-MV configuration Mach 0.90, alpha = 0, beta = 0

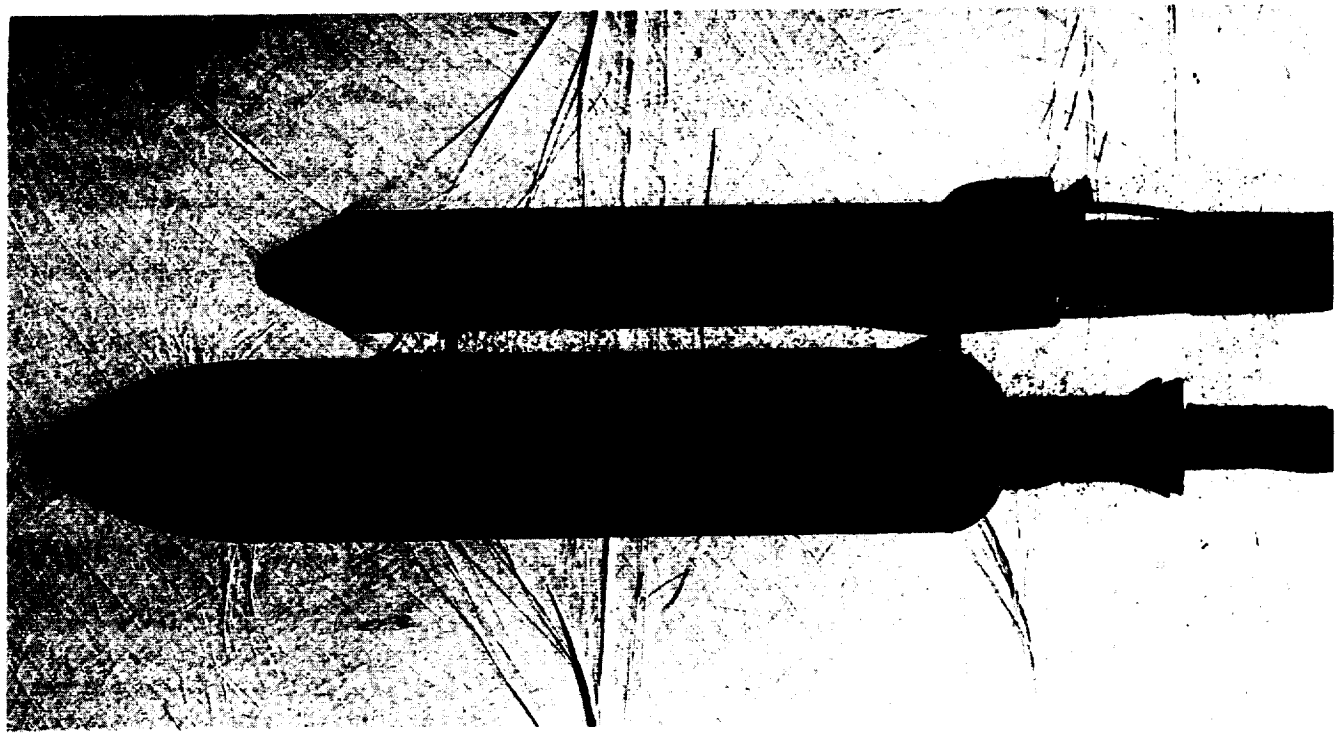

Figure 37. CYL-92-26-MV configuration Mach 0.95, alpha = 0, beta = 0

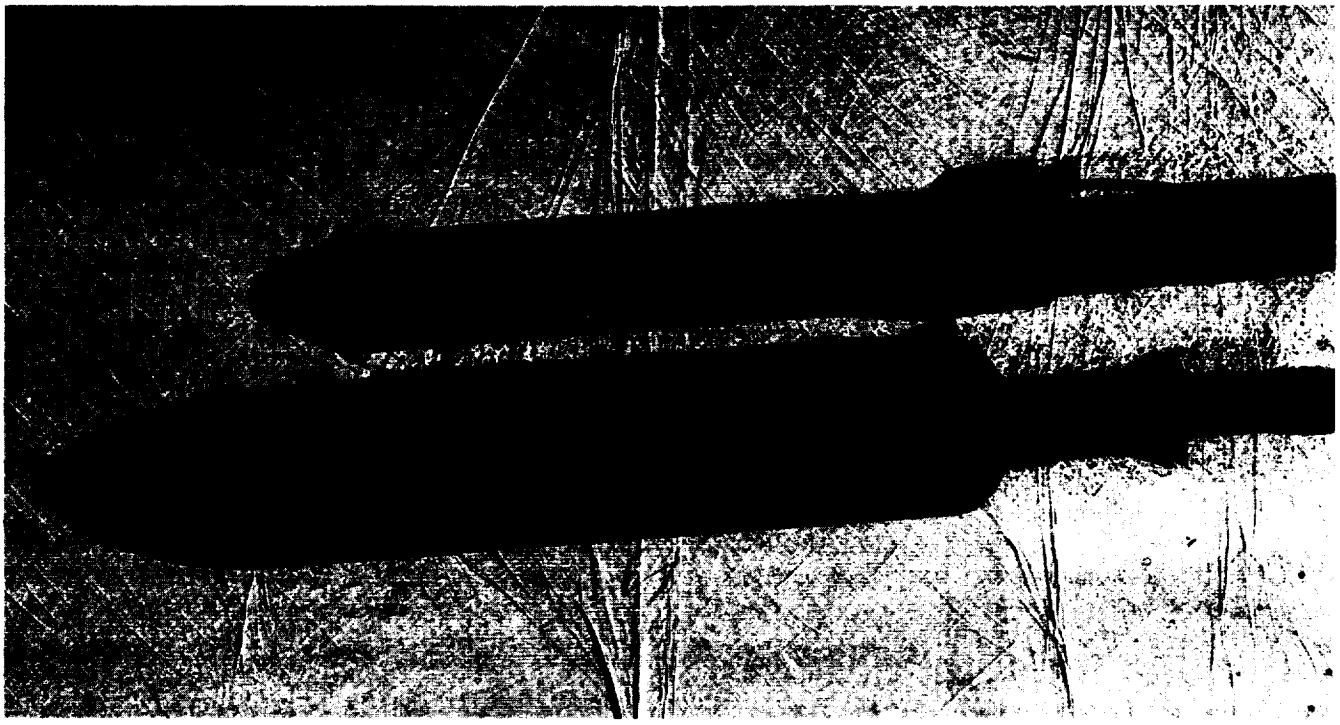

Figure 38. CYL-92-26-MV configuration Mach 0.95, alpha = -4, beta = 0

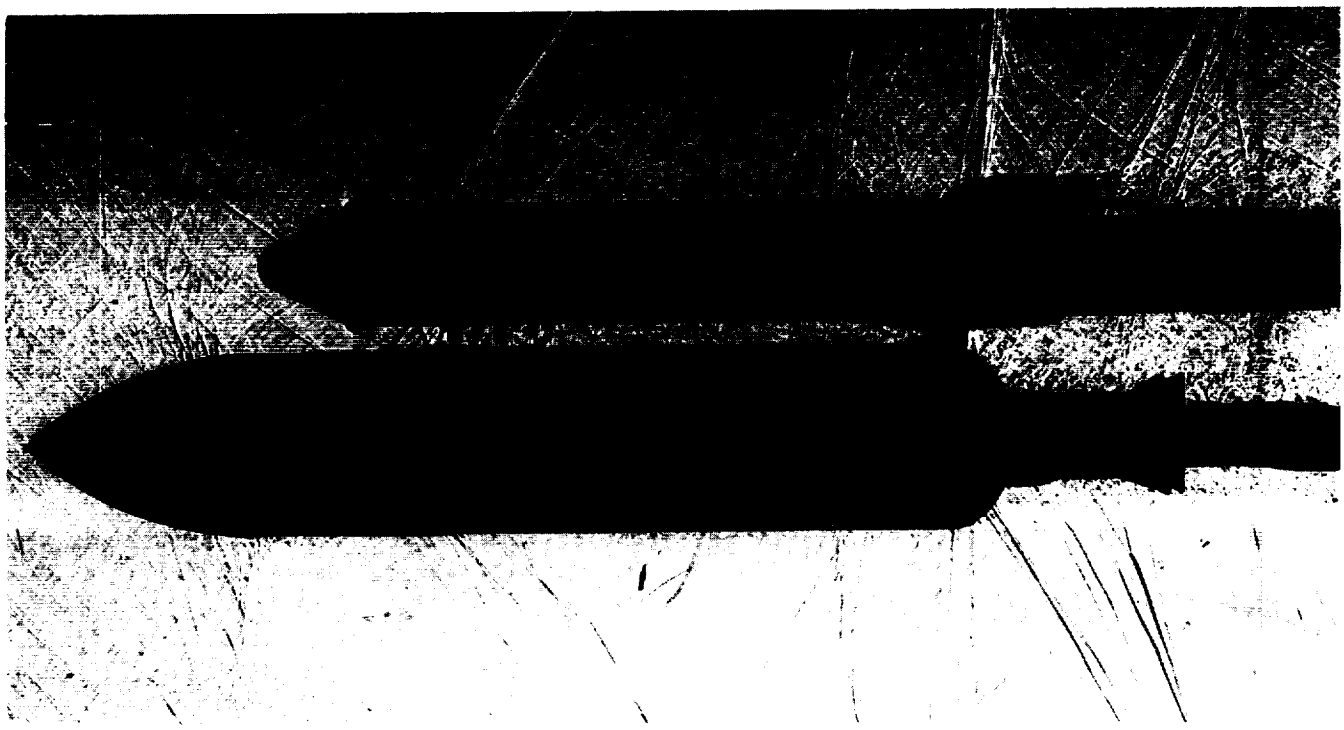

Figure 39. CYL-92-26-MV configuration Mach 1.05, alpha = 0, beta = 0

Figure 40. CYL-92-26-MV configuration Mach 1.05, alpha = -4, beta = 0

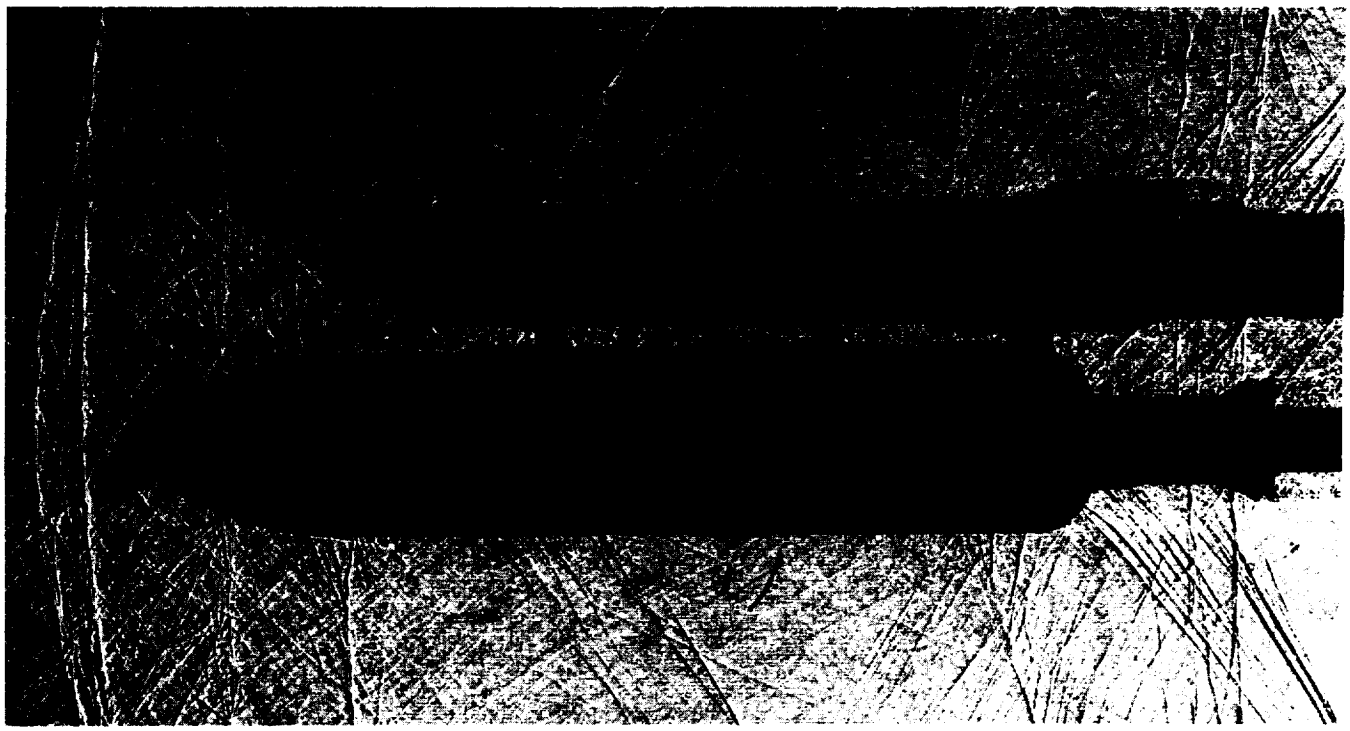

Figure 41. CYL-92-26-MV configuration Mach 1.10, alpha = 0, beta = 0

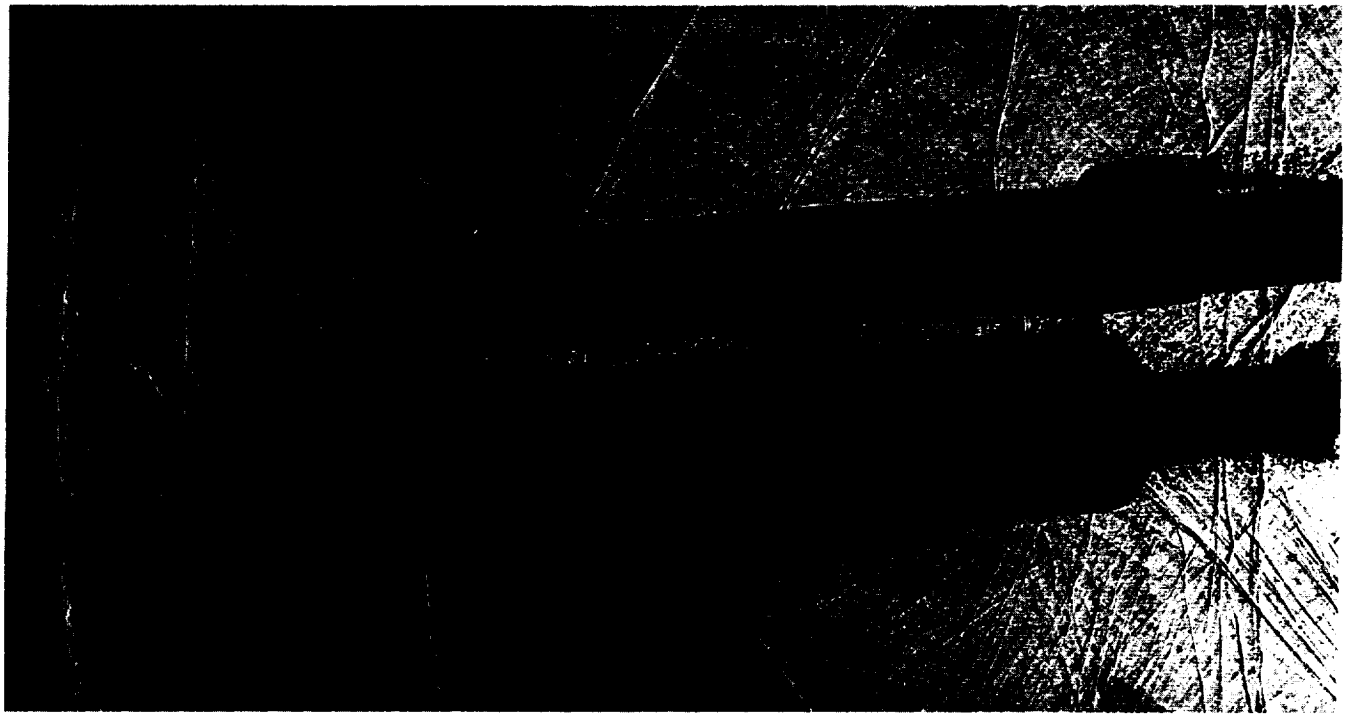

Figure 42. CYL-92-26-MV configuration Mach 1.10, alpha = -4, beta = 0

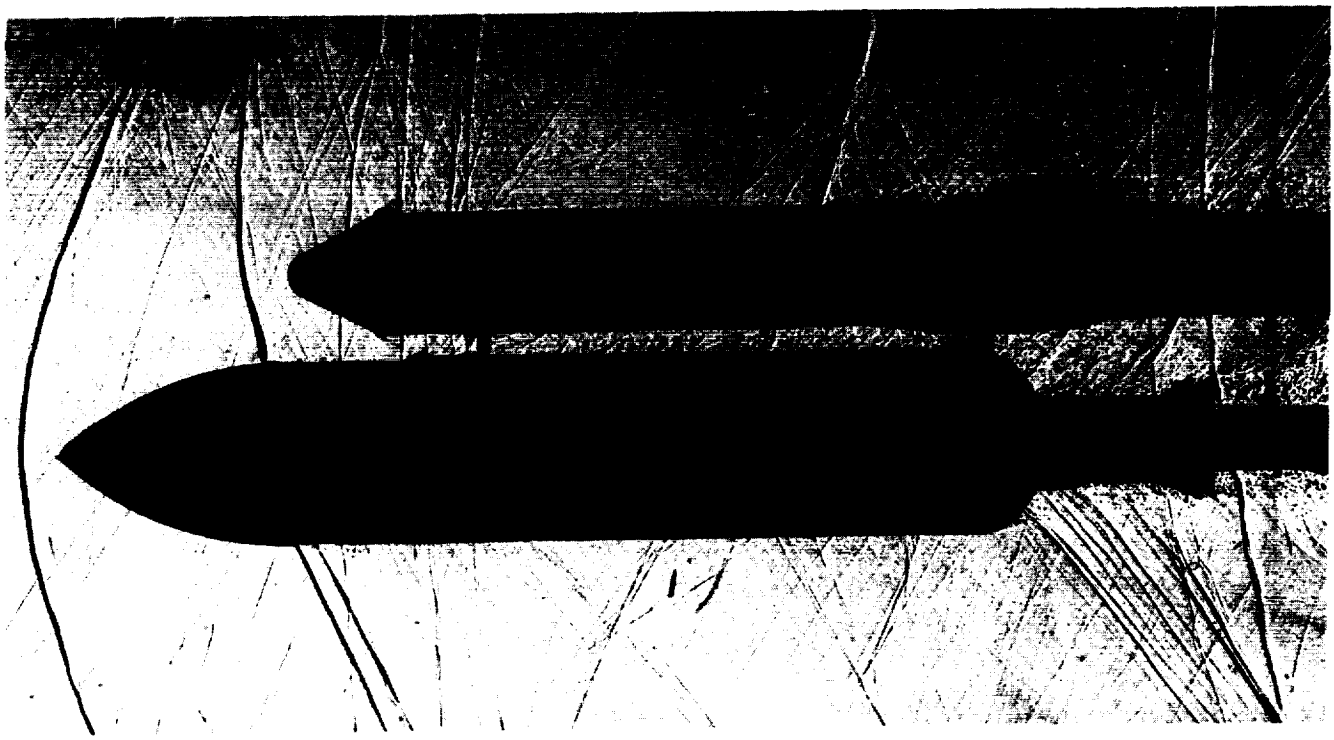

Figure 43. CYL-92-26-MV configuration Mach 1.25, alpha = 0, beta = 0

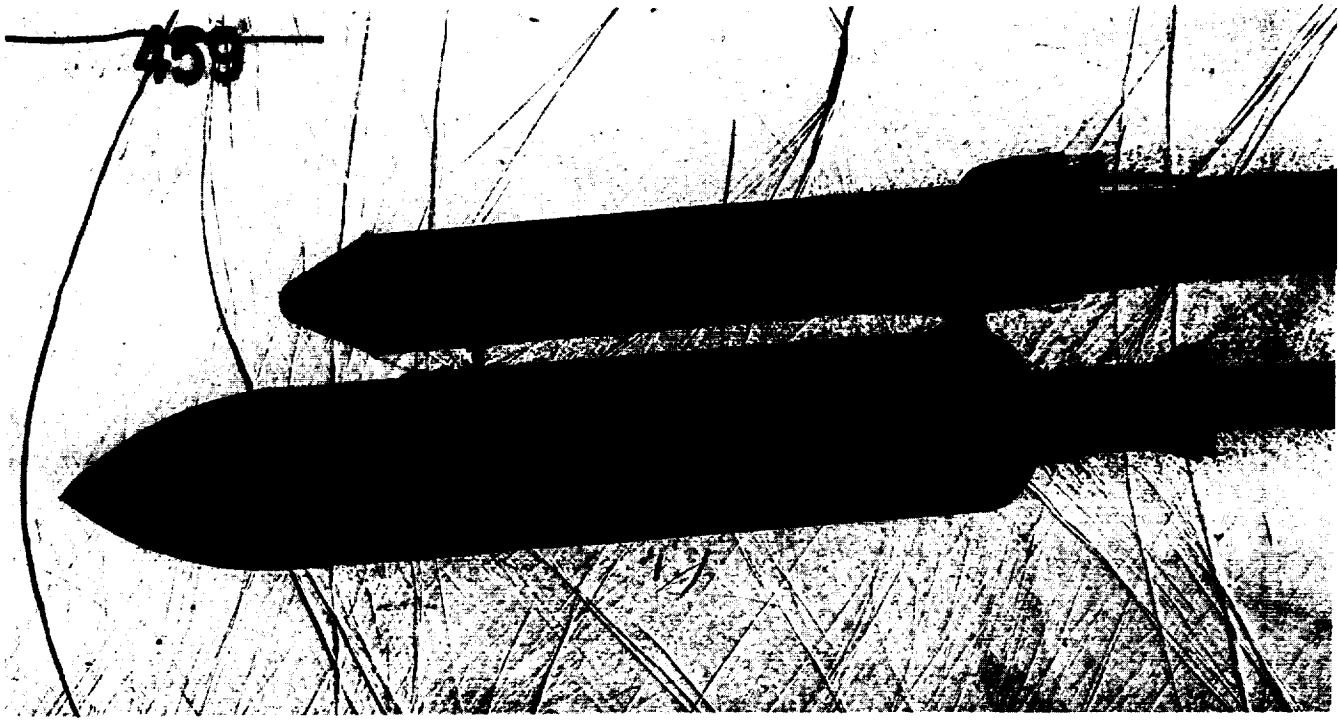

Figure 44. CYL-92-26-MV configuration Mach 1.25, alpha = -4, beta = 0

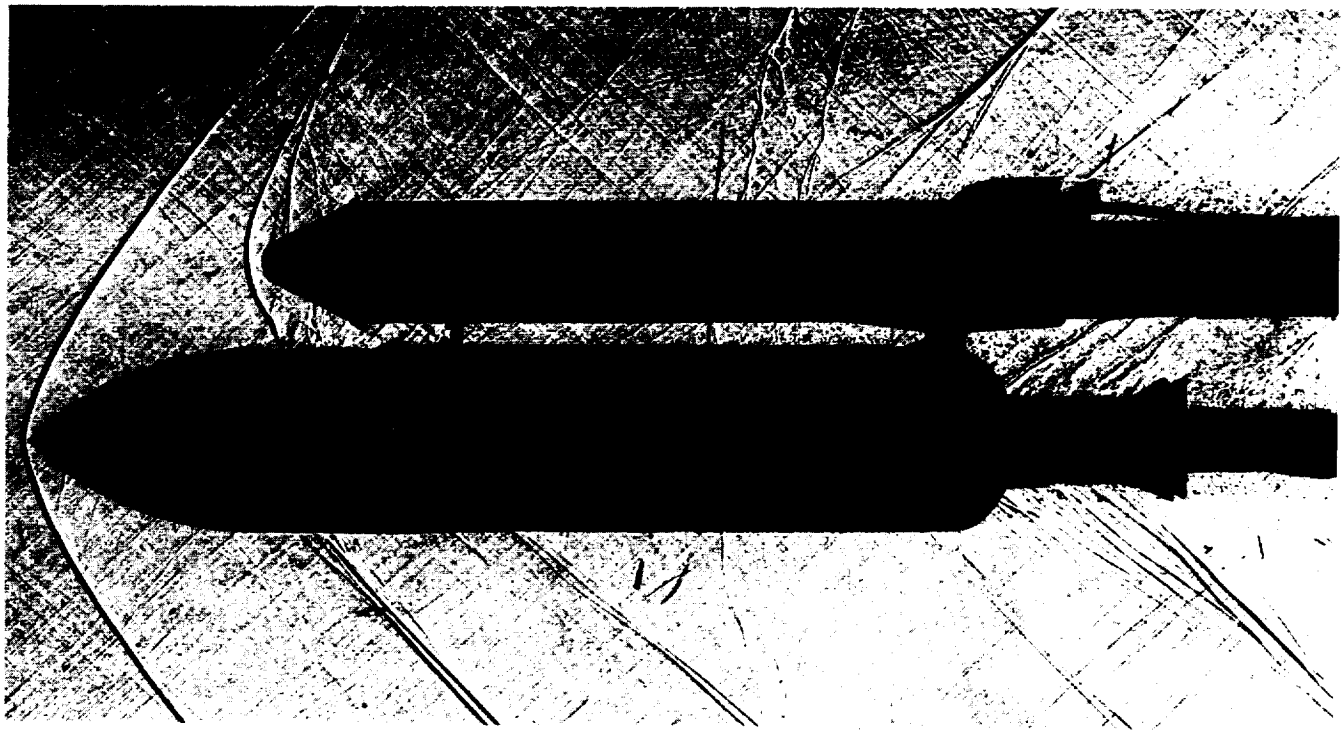

Figure 45. CYL-92-26-MV configuration Mach 1.46, alpha = 0, beta = 0

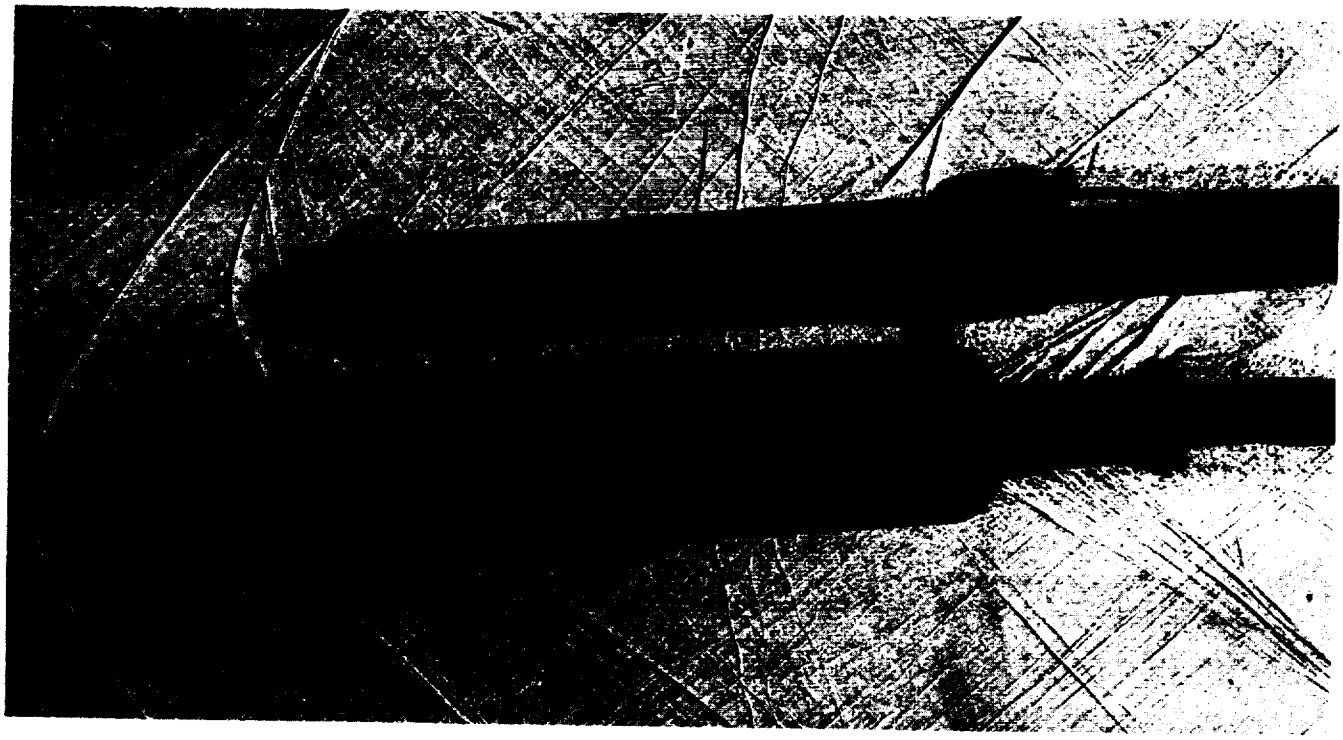

Figure 46. CYL-92-26-MV configuration Mach 1.46, alpha = -4, beta = 0

Figure 47. CYL-92-26-MV configuration Mach 1.96, alpha = 0, beta = 0

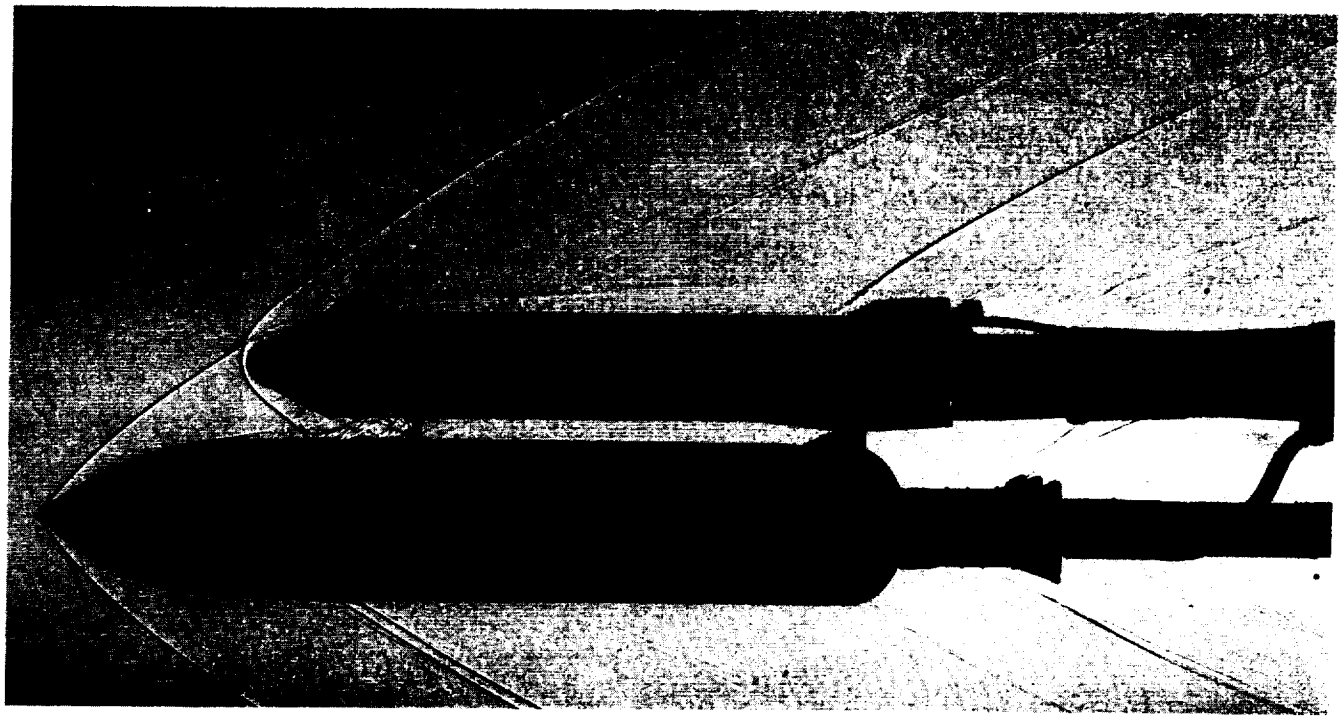

Figure 48. CYL-92-26-MV configuration Mach 2.74, alpha = 0, beta = 0

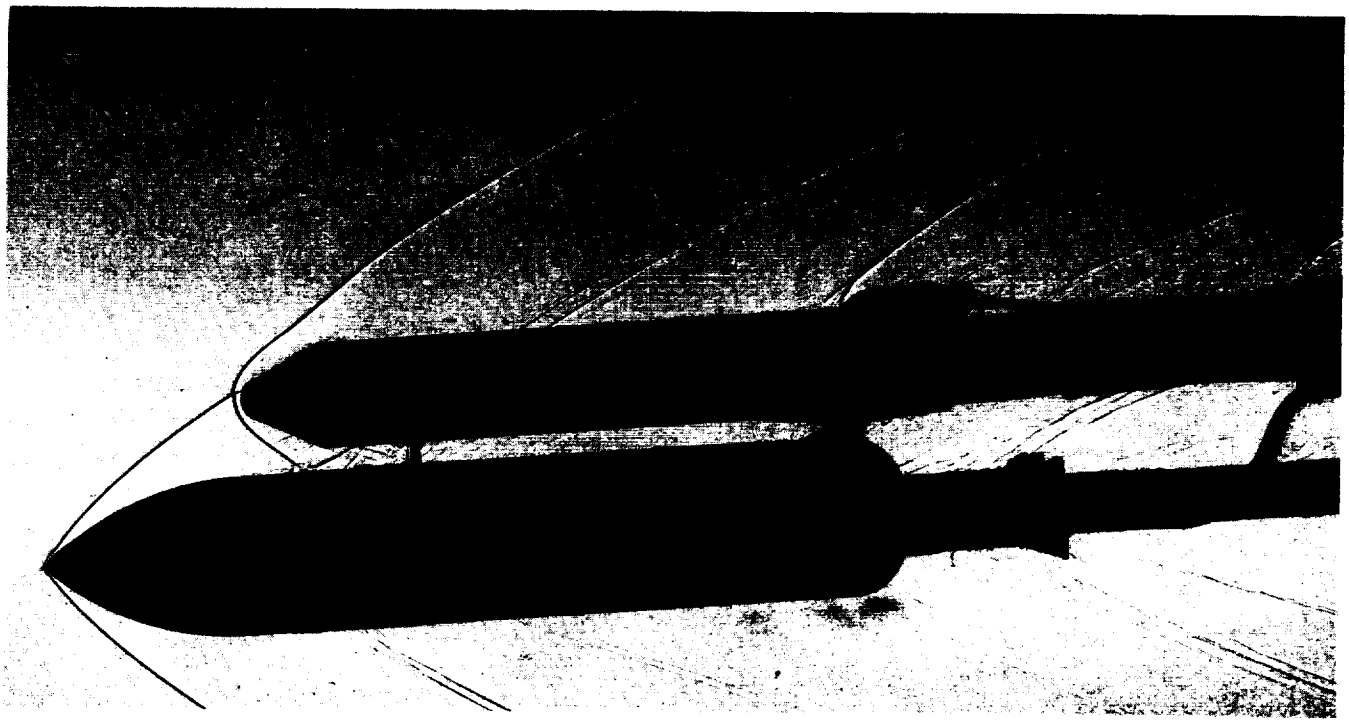

Figure 49. CYL-92-26-MV configuration Mach 2.74, alpha = -4, beta = 0

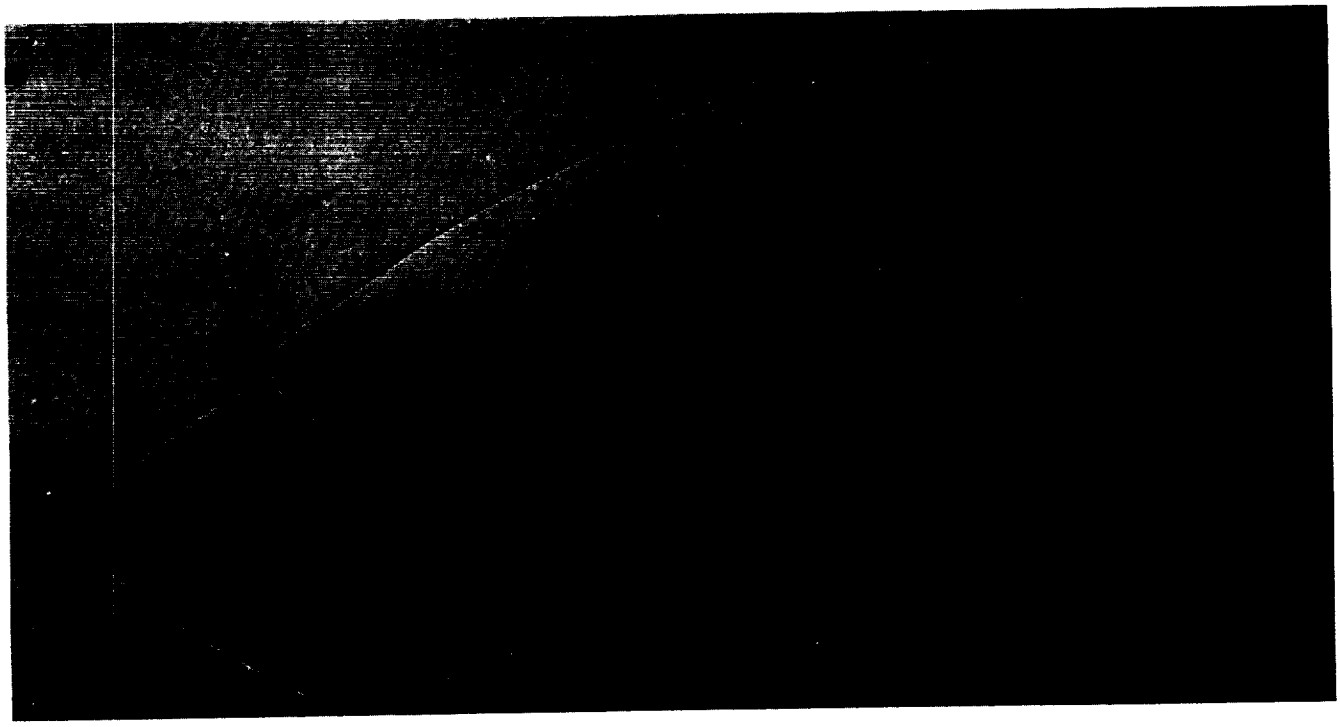

Figure 50. CYL-92-26-MV configuration Mach 3.48, alpha = 0, beta = 0

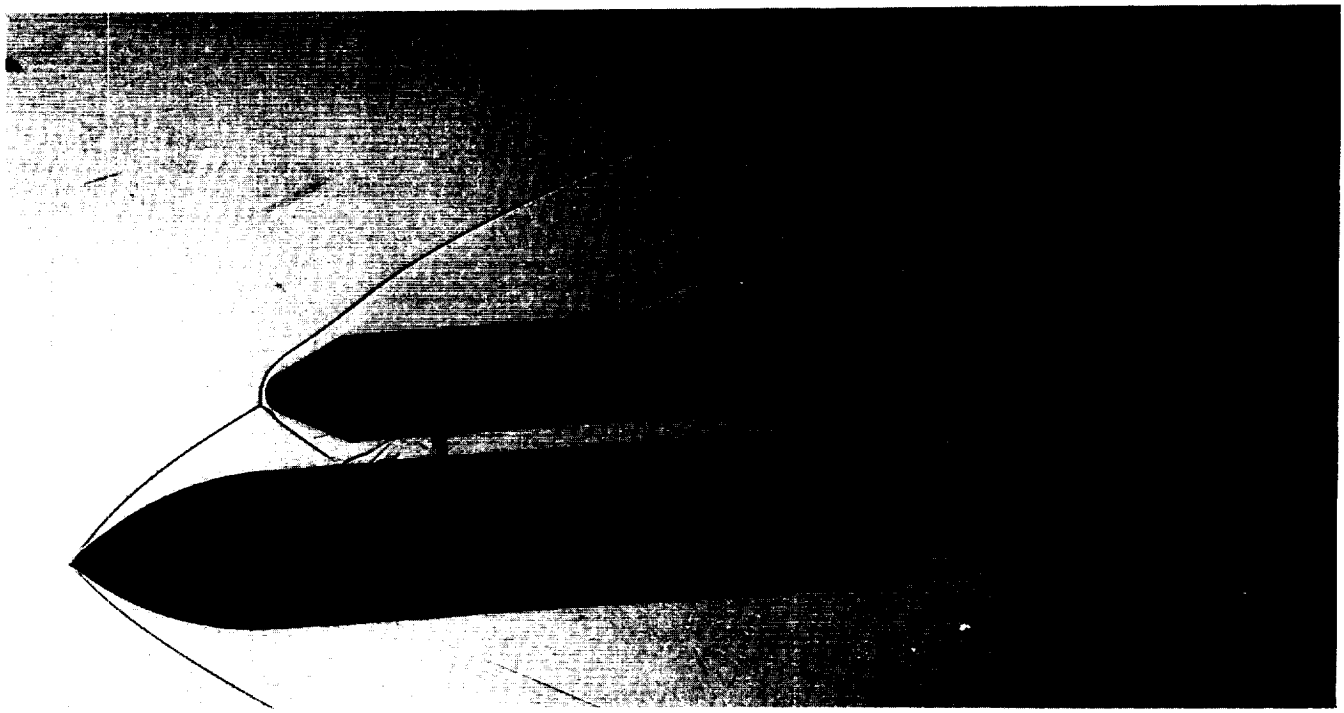

Figure 51. CYL-92-26-MV configuration Mach 3.48, alpha = -4, beta = 0

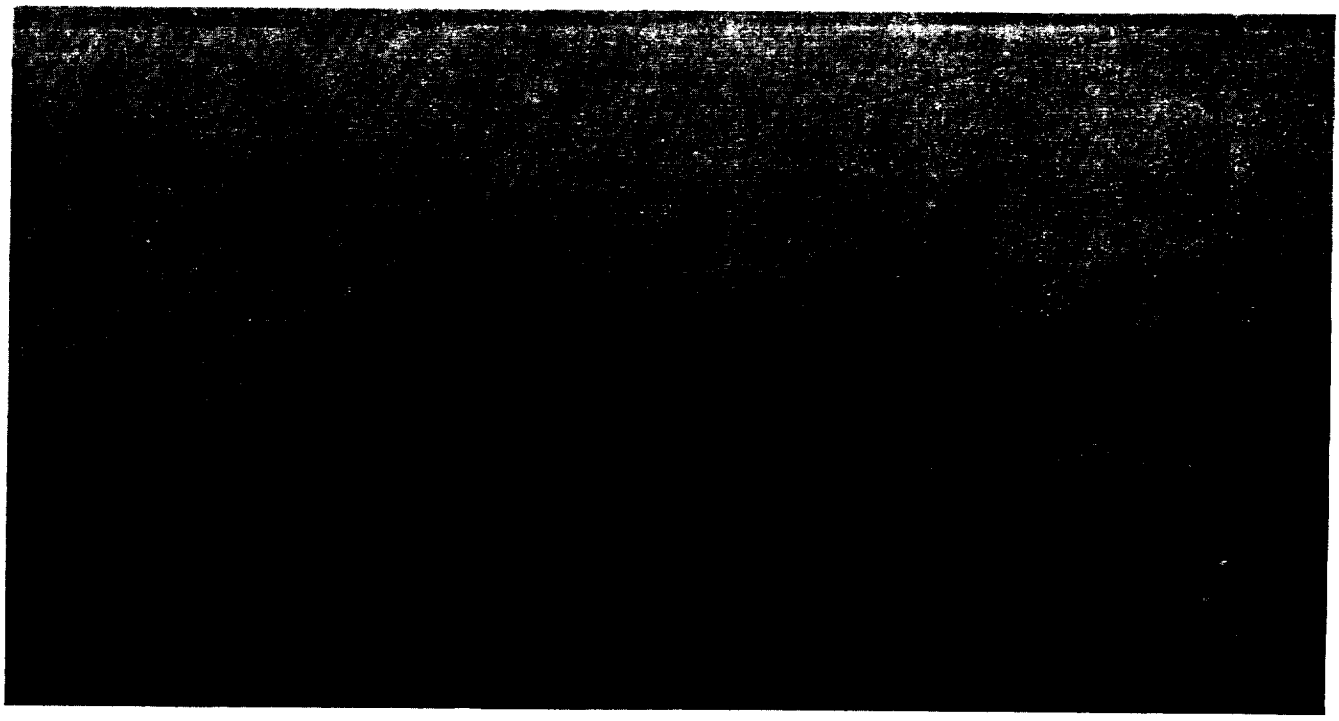

Figure 52. CYL-92-26-MV configuration Mach 4.95, alpha = 0, beta = 0

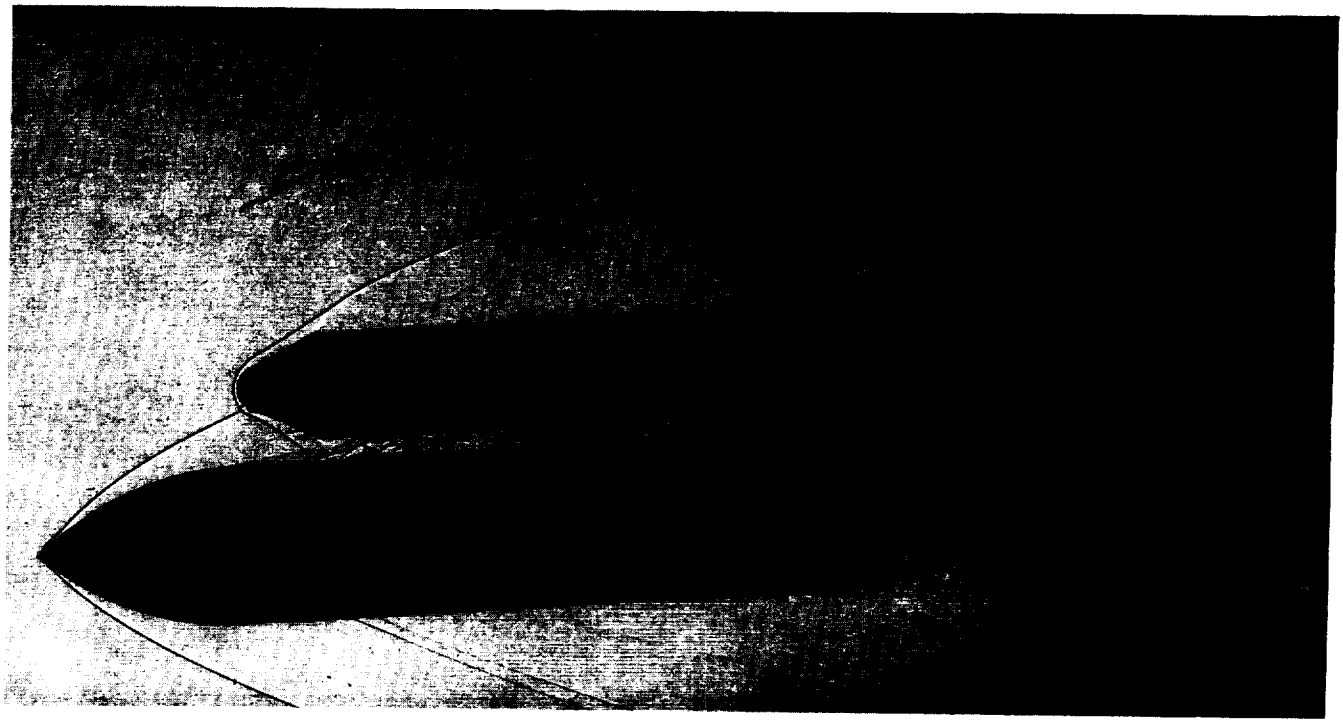

Figure 53. CYL-92-26-MV configuration Mach 4.95, alpha = -4, beta = 0

REPORT DOCUMENTATION PAGE

Form Approved
OMB No. 0704-0188

1. AGENCY USE ONLY (Leave blank)	2. REPORT DATE	3. REPORT TYPE AND DATES COVERED
	May 1993	Reference Publication

4. TITLE AND SUBTITLE

A Shadowgraph Study of Two Proposed Shuttle-C Launch Vehicle Configurations

5. FUNDING NUMBERS

6. AUTHOR(S)

A.M. Springer and D.C. Pokora

7. PERFORMING ORGANIZATION NAME(S) AND ADDRESS(ES)

George C. Marshall Space Flight Center
Marshall Space Flight Center, Alabama 35812

8. PERFORMING ORGANIZATION REPORT NUMBER

M-718

9. SPONSORING/MONITORING AGENCY NAME(S) AND ADDRESS(ES)

National Aeronautics and Space Administration
Washington, DC 20546

10. SPONSORING/MONITORING AGENCY REPORT NUMBER

NASA RP-1303

11. SUPPLEMENTARY NOTES

Prepared by Structures and Dynamics Laboratory, Science and Engineering Directorate.

12a. DISTRIBUTION/AVAILABILITY STATEMENT

Unclassified — Unlimited
Subject Category: 02

12b. DISTRIBUTION CODE

13. ABSTRACT *(Maximum 200 words)*

This report presents a shadowgraph study concerning two of the proposed Shuttle-C launch vehicle configurations. These shadowgraphs were obtained from a wind tunnel test performed in Marshall Space Flight Center's 14-in trisonic wind tunnel at various angles-of-attack and roll angles over the Mach range of 0.6 to 4.96. Variations in payload bay length were also evaluated. Major flow field phenomena can easily be seen in the shadowgraphs. Shadowgraphs are a valuable resource. They are used in the analysis of the external flow conditions the launch vehicle encounters through the ascent stage of flight. Subsequent reports will contain shadowgraph studies for other launch vehicle configurations also tested in the Marshall Space Flight Center's 14-in trisonic wind tunnel.

14. SUBJECT TERMS	15. NUMBER OF PAGES
shadowgraph, Shuttle-C, wind tunnel testing, flow visualization, launch vehicle	52
	16. PRICE CODE: A03

17. SECURITY CLASSIFICATION OF REPORT	18. SECURITY CLASSIFICATION OF THIS PAGE	19. SECURITY CLASSIFICATION OF ABSTRACT	20. LIMITATION OF ABSTRACT
Unclassified	Unclassified	Unclassified	Unlimited

NSN 7540-01-280-5500

Standard Form 298 (Rev. 2-89)
Prescribed by ANSI Std Z39-18
298-102

☆U.S. GOVERNMENT PRINTING OFFICE: 1993 - 728-064/66039

National Aeronautics and
Space Administration
Code JTT
Washington, D.C.
20546-0001

Official Business

Penalty for Private Use, $300

BULK RATE
POSTAGE & FEES PAID
NASA
Permit No. G-27

NASA

POSTMASTER: If Undeliverable (Section 158 Postal Manual) Do Not Return